

# PREPARATION AND CHARACTERIZATION OF POLY(LACTIC ACID)/RICE STRAW CELLULOSE BIO-COMPOSITE FILMS FOR PACKAGING APPLICATIONS

BY

#### SUPATTRA PIEWKLIANG

A THESIS SUBMITTED IN PARTIAL FULFILLMENT OF THE
REQUIREMENTS FOR THE DEGREE OF MASTER OF
ENGINEERING (ENGINEERING TECHNOLOGY)
SIRINDHORN INTERNATIONAL INSTITUTE OF TECHNOLOGY
THAMMASAT UNIVERSITY
ACADEMIC YEAR 2024

# THAMMASAT UNIVERSITY SIRINDHORN INTERNATIONAL INSTITUTE OF TECHNOLOGY

#### **THESIS**

BY

#### SUPATTRA PIEWKLIANG

#### **ENTITLED**

# PREPARATION AND CHARACTERIZATION OF POLY(LACTIC ACID)/RICE STRAW CELLULOSE BIO-COMPOSITE FILMS FOR PACKAGING APPLICATIONS

was approved as partial fulfillment of the requirements for the degree of Master of Engineering (Engineering Technology)

on March 18, 2025

Chairperson	Pany2.				
	(Associate Professor Chariya Kaewsaneha, Ph.D.)				
Member and Advisor	Part				
-	(Associate Professor Pakorn Opaprakasit, Ph.D.)				
Member and Co-advisor	Atotra Pet				
•	(Atitsa Petchsuk, Ph.D.)				
Member	J. Sig com				
-	(Professor Takeshi Serizawa, Ph.D.)				
Director	fles.				
	(Associate Professor Kriengsak Panuwatwanich, Ph.D.)				

Thesis Title PREPARATION AND

CHARACTERIZATION OF POLY(LACTIC

ACID)/RICE STRAW CELLULOSE BIO-COMPOSITE FILMS FOR PACKAGING

APPLICATIONS

Author Supattra Piewkliang

Degree Master of Engineering (Engineering

Technology)

Faculty/University Sirindhorn International Institute of Technology/

Thammasat University

Thesis Advisor Associate Professor Pakorn Opaprakasit, Ph.D.

Thesis Co-Advisor Atitsa Petchsuk, Ph.D.

Academic Years 2024

#### **ABSTRACT**

The development of sustainable and biodegradable poly(lactic acid) (PLA) biocomposite films using cellulose fibers extracted from rice straw (RSC), a major agricultural waste product in Southeast Asia. This study tackles pressing environmental issues arising from the excessive use and improper disposal of petroleum-based plastics, focusing on single-use applications such as food packaging. Rice straw cellulose was extracted through a chemical process involving alkaline, bleaching, and acidic treatments, resulting in cellulose fibers with enhanced purity. These cellulose fibers were subsequently modified with alkyl ketene dimer (AKD), a cost-effective and hydrophobic reagent with food-safe properties. Eco-friendly, solvent-free ball-milling and thermal treatment processes were employed to improve their compatibility with the hydrophobic PLA matrix. The success modification was verified by Fourier-transform infrared (FTIR) spectroscopy, demonstrating the reaction between the lactone ring of AKD and hydroxyl groups (-OH) of cellulose successfully generated  $\beta$ -ketoester bonds, reflected by a new band at 1735 cm<sup>-1</sup>, which imparted hydrophobic characteristics to the cellulose surface and improved dispersion within the PLA matrix.

The PLA/RSC bio-composite films were prepared using a solvent-casting method with cellulose fiber contents varying between 1-7 %wt. The films' mechanical properties, water vapor permeability (WVP), and hydrophobicity (water contact angle) were investigated. The results indicated significant improvements in mechanical properties, including tensile strength and elongation at break, particularly at a 3 %wt loading of the AKD-modified cellulose. The films also exhibited enhanced hydrophobicity, with water contact angles increasing to 91.5°, demonstrating improved water resistance compared to neat PLA films. Furthermore, the inclusion of modified cellulose maintained the water vapor permeability of the films, ensuring their suitability for packaging applications that require effective moisture control. By transforming rice straw into high-performance bio-composite films, this research promotes a bio-circular economy, reduces environmental pollution, and creates value-added products. Moreover, the developed PLA/RSC bio-composite films present a promising ecofriendly for smart packaging applications.

**Keywords**: Poly(lactic acid), Rice straw cellulose, Alkyl ketene dimer, Ball-milling, Bio-composite, Packaging film

#### **ACKNOWLEDGEMENTS**

I wish to acknowledge the Thailand Advanced Institute of Science and Technology and Tokyo Institute of Technology (TAIST Tokyo Tech), Sirindhorn International Institute of Technology (SIIT), and the Center of Excellence in Functional and Advanced Materials Engineering (CoE FAME), Thammasat University, for their financial support, which has enabled me to pursue my research.

I express my deepest gratitude to my advisor, Associate Professor Dr. Pakorn Opaprakasit, for his unwavering support, insightful guidance, and invaluable expertise throughout my research journey. Your encouragement and belief in my abilities have been a constant source of motivation. I would like to give my sincere gratitude to my co-advisor, Dr. Atitsa Petchsuk, National Metal and Materials Technology Center (MTEC), National Science and Technology Development Agency (NSTDA). I appreciate all your support through words of encouragement or valuable advice. I have learned many laboratory skills to help me become a good researcher. I am immensely grateful to the members of my thesis committee, Associate Professor Dr. Chariya Kaewsaneha and Professor Dr. Takeshi Serizawa from the Tokyo Institute of Technology, for their constructive feedback and thoughtful suggestions and for taking the time to review my work. Their insights have significantly contributed to the quality of this thesis.

I am also grateful to the laboratory engineer, Ms. Neungruthai Tippo, for her assistance and resources, which have been vital to this project. Special thanks to my friends and seniors, Dr. Narisara Jaikaew, Dr. Kamonchanok Thananukul, and Mr. Pattara Somnuk, for their collaboration, stimulating discussions, and camaraderie during this journey. Your support has made challenging moments much easier to overcome. I sincerely thank my family for their unwavering love, encouragement, and patience, which have served as my foundation. Their unwavering support and belief in me have been a continuous source of strength throughout this journey.

Supattra Piewkliang

## **TABLE OF CONTENTS**

	Page
ABSTRACT	(1)
ACKNOWLEDGEMENTS	(3)
LIST OF TABLES	(6)
LIST OF FIGURES	(7)
LIST OF SYMBOLS/ABBREVIATIONS	(10)
CHAPTER 1 INTRODUCTION	
1.1 General Background	1
1.2 Objectives	4
1.3 Scope of the study	4
CHAPTER 2 REVIEW OF LITERATURE	6
2.1 Biopolymer	6
2.2 Poly(lactic acid) (PLA)	10
2.3 PLA bio-composite	11
2.4 Cellulose	15
2.5 Rice straw	18
2.6 Alkyl ketene dimer	19
2.7 Ball milling	23
CHAPTER 3 EXPERIMENTAL APPROACH	25
3.1 Materials	26
3.2 Experimental	26
CHAPTER 4 RESULTS AND DISCUSSION	30

	(5)
CHAPTER 5 CONCLUSION	52
5.1 Conclusion	52
5.2 Suggestion and recommendation	52
REFERENCES	53
BIOGRAPHY	59

# LIST OF TABLES

Tables	Page
2.1 Mechanical and gas barrier properties of PLA bio-composite	14
2.2 Extraction methods, diameter, and percentage composition of	
cellulose's chemical components from various natural sources	17



## LIST OF FIGURES

Figures	Page
1.1 Plastic waste generation by sector in 2018	1
2.1 Classification of biopolymers	7
2.2 Pictorial view of the PLA bottles exposed at 30 day of compost conditions	7
2.3 Visual aspect of plasticized PLA and PLA-PHB films at different	
disintegration times	8
2.4 Vegetable rate of water loss a) control, b) PVA and	
c) 0.6(MWCNTs-ZnO)/PVA	9
2.5 Multifunctional cellulose-lignin films (LRCPL30-3) applied as packaging	
materials for shrimp	10
2.6 Synthesis of poly(lactic acid)	10
2.7 Isomers of lactic acid	11
2.8 Structure of cellulose	15
2.9 Comparison of rice straw burning and production in each country	19
2.10 Structure of alkyl ketene dimer (AKD)	19
2.11 Reaction of cellulose treated with AKD	20
2.12 Water contact angle of treated wood and FTIR spectra of neat AKD (A),	
untreated teakwood (B), and teakwood samples treated with	
AKD@SDS (C) and AKD@PC (D)	21
2.13 Effect of relative humidity on water vapor permeability of AUC	
and AUC-AKD0.1 films	21
2.14 SEM images of the fractured surface of the composites: (a),	
neat PLA; (B), PLA with AKD; (C), NF filled PLA; (D), NF filled	
PLA with AKD; (E), GF filled PLA; (F), GF filed PLA with AKD;	
(G), NF and GF filled PLA with AKD. AKD, alkyl ketene dimer; PLA,	
poly(lactic acid)	22
2.15 The modification of surface cellulose nanofibers with esterification	
through ball milling	24
3.1 The overall process of (a) extraction of RSC, (b) RSC surface	
modification, and 1(c) fabrication of PLA/RSC bio-composite films	25

	(8)
3.2 The procedure for the extraction process	26
3.3 The overall procedure for the AKD-treated RSC and their characterization	28
4.1 FTIR spectrum of extracted RSC	31
4.2 SEM images of the extracted RS (a, b) original fiber,	
(c, d) alkaline treatment, (e, f) bleaching, (g, h) acidic treatment	32
4.3 ATR-FTIR spectra of the extracted RSC (a) original fiber,	
(b) alkaline treatment, (c) bleaching, and (d) acidic treatment	33
4.4 ATR-FTIR Spectrum of (a) MCC and (b) RSC	35
4.5 FTIR spectrum of neat AKD	36
4.6 The chemical reaction of AKD-treated cellulose surface	36
4.7 ATR-FTIR spectra of MCCD various reaction times	37
4.8 ATR-FTIR spectra of (a) neat AKD, (b) RSC, (c) RSCD after ball milling,	
and (d) RSCD after heating at 110 °C	38
4.9 ATR-FTIR spectra of (a) RSCD before and (b) after washing with THF	39
4.10 SEM images of (a) RSC, (b) RSC after ball milling, (c) RSCD after	
heating at 110 °C, (d) MCC, (e) MCC after ball milling, and (f) MCCD	
after heating at 110 °C	40
4.11 Stress-strain curves of PLA/long and short RSC bio-composite films	
at various fiber contents	41
4.12 Tensile strength of PLA/long and short RSC bio-composite films	
at various fiber contents	42
4.13 Young's modulus of PLA/long and short RSC bio-composite films	
at various fiber contents	42
4.14 Elongation at break of PLA/long and short RSC bio-composite films	
at various fiber contents	43
4.15 Stress-strain curves of PLA/RSC, RSCD, and AKD bio-composite	
films at various fiber contents	44
4.16 Tensile strength of PLA/RSC, RSCD, and AKD bio-composite films	
at various fiber contents	45
4.17 Young's modulus of PLA/RSC, RSCD and AKD bio-composite	
films at various fiber contents	45

	(9)
4.18 Elongation at break of PLA/RSC, RSCD and AKD bio-composite	
films at various fiber contents	46
4.19 Stress-strain curves of PLA/RSCD and MCCD bio-composite films	
at various fiber contents	47
4.20 Tensile strength of PLA/RSCD and MCCD bio-composite films at	
various fiber contents	47
4.21 Young's modulus of PLA/RSCD and MCCD bio-composite films	
at various fiber contents	48
4.22 Elongation at break of PLA/RSCD and MCCD bio-composite films	
at various fiber contents	48
4.23 Cross-section image of (a, b) PLA/RSC and (c, d) PLA/RSCD bio-based	
composite films at 3 %wt.	49
4.24 Water vapor permeability of PLA/RSC bio-composite films at	
various fiber contents	50
4.25 Water contact angle of PLA/RSC and RSCD bio-composite films	
at various fiber contents	51
4.26 WCA images of PLA/RSC and RSCD bio-composite films at	
various RSC contents	51

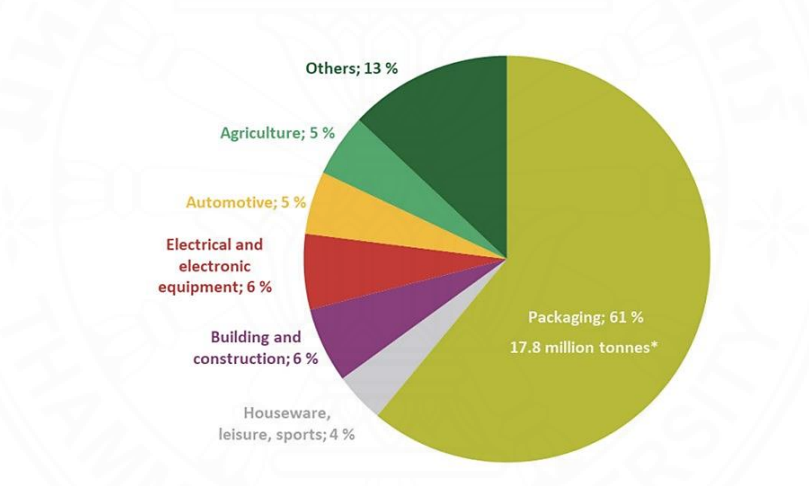
# LIST OF SYMBOLS/ABBREVIATIONS

Terms
Poly(lactic acid)
Rice straw
Rice straw cellulose
Microcrystalline cellulose
Alkyl ketene dimer
RSC modified with AKD
MCC modified with AKD
Tetrahydrofuran
Sodium hydroxide
Hydrogen peroxide
Hydrochloric acid

# CHAPTER 1 INTRODUCTION

#### 1.1 General Background

In recent decades, waste from single-use packaging plastics become one of the major environmental pollutions due to its high consumption rate. Many petroleum-based plastics, such as polystyrene (PS), polyethylene terephthalate (PET), polyamide (PA), polypropylene (PP), and polyethylene (PE), are commercially used in packaging applications. Food packaging accounts for 61% of total plastic waste, as reported by ECA based on data from 'A circular economy for plastic – A European Overview,' Plastics Europe, 2019. Year 2018, as shown in Figure 1.1.



\* Total post-consumer plastic waste collected via relevant streams - 29.1 million tonnes

**Figure 1.1** Plastic waste generation by sector in 2018.

(Source: ECA based on data from 'A circular economy for plastic – A European Overview,' Plastics Europe, 2019.)

Conventional plastics offer a favorable combination of high flexibility, mechanical strength, durability, high gas/moisture permeability, transparency, and ease of processing, making them suitable for food packaging. Although petroleum-based plastics have benefits, they are mostly non-degradable, persisting in the environment for years and causing significant harm. Consequently, extensive research regarding environmentally friendly and sustainable packaging has been conducted. Among all

approaches, the use of biopolymers become a promising approach to reduce the negative impacts of plastic wastes, owing to biodegradability, renewability, and low energy consumption. Examples of such polymers include poly(lactic acid) (PLA), poly(butylene succinate) (PBS), polyhydroxyalkanoates (PHA), and starch. (Bordes et al., 2009; Kumar et al., 2019). Among various biopolymers, PLA is extensively studied due to its exceptional biodegradability, renewability, high mechanical strength, ease of processing, and superior optical properties. PLA is a biopolymer derived from renewable resources such as corn, sugarcane, and starch, making it a sustainable alternative to conventional plastics. Its versatility enables its use in various applications, including packaging, 3D printing filaments, and biomedical products. However, its poor mechanical and barrier properties have limited its application in some areas. To overcome these limitations and widen its applications, many researchers have developed PLA-based composites by incorporating natural fibers, such as cellulose and starch, into PLA matrix to improve its properties (Abdulkhani et al., 2014; Ilyas et al., 2021).

Cellulose fiber is a natural fiber derived from plants, such as wood, cotton, and wheat. In plant cell walls, cellulose chains are bound together by hydrogen bonds, forming cellulose microfibrils, which serve as the fundamental structural units of plant fibers (Nasri-Nasrabadi et al., 2014). Additionally, cellulose can also be derived from agricultural waste, such as rice straw, rice bran, and palm oils, which can be extracted and utilized. Rice straw constitutes an essential agricultural waste in Southeast Asia, particularly in Thailand, where the annual production exceeds 20 million tons. Unfortunately, during peak seasons of rice harvesting, a substantial portion of this biomass remains unutilized and is frequently subjected to burning. As a result, approximately 90% of rice straw is burning as a means of disposal, leading to grave environmental issues on both local and global scales (Kophimai et al., 2020). Hence, the objective of this research is to extract cellulose fiber from rice straw as a solution to mitigate these problems. By utilizing the potential of cellulose fiber extraction, aim for unutilized rice straw waste and pave the way for sustainable resource management. Cellulose fiber can be used as reinforcing fillers for many polymers to enhance their mechanical properties but retain biodegradability. This is owing to its low cost, low density, non-toxicity, fire resistance, non-abrasiveness, and biodegradability. Although

cellulose holds significant promise as a biological reinforcement in bio-composites, its dispersion within hydrophobic matrices remains challenging due to its strong affinity for water, attributed to the high concentration of hydroxyl groups in its chemical structure. Thus, many surface modification methods, e.g., physical and chemical treatments, have been used to promote interfacial interaction between polymer matrix and cellulose surfaces (Abdulkhani et al., 2014).

Among all surface modifying agents, Alkyl ketene dimer, commonly known as AKD, is a promising modifying agent for hydroxyl-rich materials due to its high reactivity toward chemical reactions with hydroxyl groups (-OH), especially cellulose (Ali Varshoei, 2013). The interaction between the lactone ring of AKD and the hydroxyl groups of cellulose results in the formation of a  $\beta$ -ketoester bond on the cellulose surface, where the hydrophobic tails align as hydrophobic side chains (Kaewsaneha et al., 2022). AKD is commonly utilized as a cost-effective neutral sizing agent in the paper industry to enhance the water resistance of paper due to its high hydrophobicity. Furthermore, AKD is considered a food-safe material, as it is derived from fatty acids containing an unsaturated  $\beta$ -lactone ring and alkyl chains with 16–18 carbon atoms.

In this work, PLA-based bio-composites with high water vapor permeability and hydrophobicity properties are developed. Cellulose fibers are extracted from low-cost rice straw derived from agricultural waste. An eco-friendly and solvent-free modifying process is applied to prepare modified cellulose fiber, improving compatibility between the cellulose fibers and the PLA matrix. The chemical reaction between the AKD and cellulose was confirmed by an attenuated total reflectance Fourier transform infrared (ATR-FTIR) spectroscopy. The PLA/RSC bio-composite films were prepared using the solvent casting method. The contents of cellulose fiber were varied at 1, 3, 5, and 7 %wt. The water vapor permeability (WVP), hydrophobicity (water contact angle), and mechanical properties of the PLA/RSC bio-composite films are investigated. The material is aimed at use in smart packaging films. The films are expected to be completely compostable, biodegradable, and useful for various applications. The use of waste materials to create a good quality product could promote a bio-circular economy with the utilization of natural resources and positive benefits to society and the country.

#### 1.2 Objectives

- 1. Develop biodegradable packaging films from PLA/cellulose bio-composite.
- 2. Extract cellulose fibers from rice straw and further use them as reinforcing filler for PLA.
- 3. Modify a cellulose surface by employing chemical reactions among the hydroxyl (-OH) groups of cellulose and lactone ring of alkyl ketene dimer (AKD).
- 4. Develop an eco-friendly and solvent-free modifying process using ball-milling and thermal treatment.
- Investigate the effect of filler contents on water vapor permeability (WVP), hydrophobicity (water contact angle), and mechanical properties of the PLA bio-composite films.

#### 1.3 Scope of the study

#### Part I Extraction and characterization of rice straw cellulose

- 1. Extraction of rice straw cellulose (RSC) fibers from rice straw (RS) using alkaline treatment, bleaching, and acidic treatment.
- 2. Investigated chemical structure and morphology of the extracted rice straw cellulose (RSC) using Fourier-transform infrared (FTIR) spectroscopy and scanning electron microscope (SEM), respectively.

#### Part II Preparation of RSC treated with AKD

- Finding optimum conditions for Alkyl ketene dimers (AKD) treated RSC using microcrystalline cellulose (MCC) by varying the treatment time and AKD content.
- 2. Modify the RSC with AKD (RSCD) by using the ball-milling machine and heating at 110 °C for 15 h for further use as reinforcing fillers for the commercial PLA.

3. Study and confirm the chemical reaction among the hydroxyl (-OH) groups of cellulose and lactone ring of alkyl ketene dimer (AKD) using Fourier-transform infrared (FTIR) spectroscopy.

#### Part III Fabrication and characterization of PLA/RSC bio-composite films

- 1. Apply the modified cellulose as a reinforcing material for PLA by solvent casting method, the filler contents content is varied at 1, 3, 5, and 7 %wt.
- 2. Investigate the mechanical, morphology, hydrophobicity, and water vapor permeability of the PLA compared to PLA/modified RSC bio-composite films.

#### **CHAPTER 2**

#### **REVIEW OF LITERATURE**

While many conventional plastics, such as PA, PP, PET, PE, and PS, have considerable potential for mechanical recycling, their recycling processes are economically unfavorable due to the high costs associated with sorting and cleaning. This challenge represents a major obstacle to the widespread implementation of plastic recycling initiatives (Marano et al., 2022; Talegaonkar et al., 2017). Alternatively, biopolymers have raised global attention for packaging materials, surpassing petroleum-based polymers, owing to their biodegradability, renewability, and lower energy consumption (Perera et al., 2023). To address these challenges, biopolymers have emerged as a promising solution for sustainable food packaging (Kumari et al., 2022).

#### 2.1 Biopolymers

Biopolymers, also known as biodegradable polymers, originate from renewable natural sources, including plants, animals, and microorganisms, and can also be synthetically produced using raw materials such as starch, sugars, oils, and natural fats (Basavegowda & Baek, 2021; Ncube et al., 2020). Biopolymers, as illustrated in Figure 2.1, can be categorized into various types depending on the source of the raw materials and the methods used for production. These categories encompass:

- (i) Natural biopolymers, which consist of plant-derived carbohydrates like starch, cellulose, chitosan, alginate, agar, and carrageenan, alongside proteins sourced from animals or plants such as soy protein, corn zein, wheat gluten, gelatin, collagen, whey protein, casein, among others.
- (ii) Synthetic biodegradable polymers including poly(lactic acid) (PLA), poly(glycolic acid) (PGA), poly(caprolactone) (PCL), poly(butylene succinate) (PBS), poly(vinyl alcohol) (PVA), and similar materials.
- (iii) Biopolymers synthesized through microbial fermentation, such as microbial polyesters like poly(hydroxyalkanoates) (PHAs), which encompass

poly(hydroxybutyrate) (PHB), as well as microbial polysaccharides like pullulan and curdlan (Rhim et al., 2013; Talegaonkar et al., 2017).

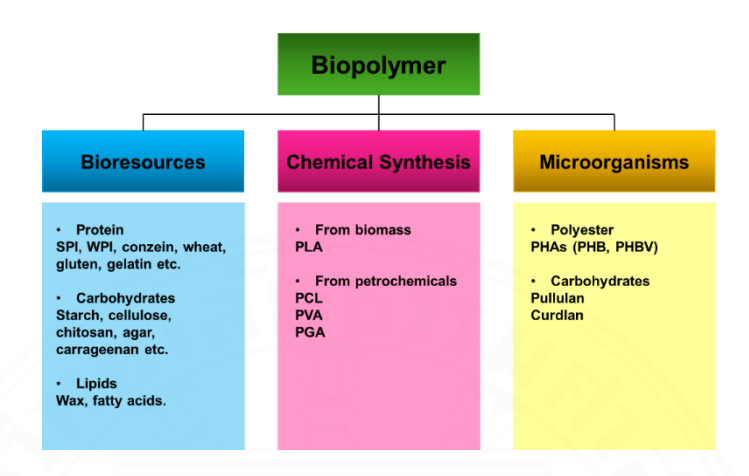
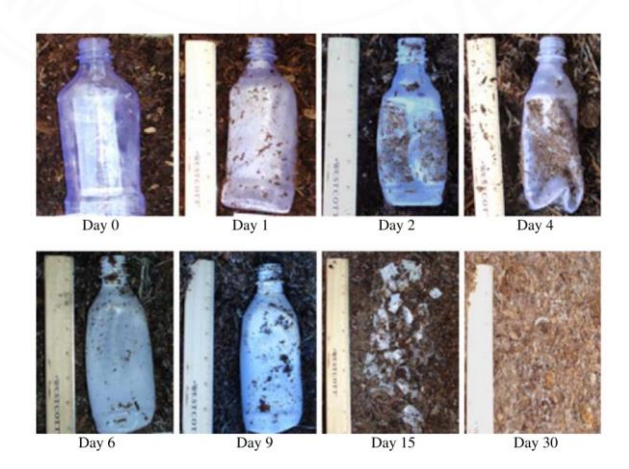


Figure 2.1 Classification of biopolymers. (adapted from Rhim et al. (2013))

Much research has been conducted on applying biopolymers as packaging due to their biocompatibility, biodegradability, environmentally friendly, and non-toxicity. In 2006, Kale et al. successfully investigated the decomposition of commercially available PLA-based biodegradable packaging under real composting conditions over a 30-day period. The results indicate that the PLA packaging degraded after less than 30 days, as illustrated in Figure 2.2.



**Figure 2.2** Pictorial view of the PLA bottles exposed at 30 day of compost conditions. (Kale et al., 2006)

Subsequently, Arrieta et al. successfully fabricated films for food packaging of poly(lactic acid) and poly(hydroxybutyrate) blends (PLA-PHB) by including two distinct plasticizers, poly(ethylene glycol) (PEG) and acetyl-tri-n-butyl citrate (ATBC). A laboratory-scale composting test was conducted to examine the degradation of PLA-PHB films at a controlled temperature of 58±2 °C over 28 days. The findings reveal that blending PLA with PHB slows down the degradation process compared to pure PLA. Conversely, incorporating plasticizers into PLA accelerates its degradation, completing within 28 days, as illustrated in Figure 2.3.

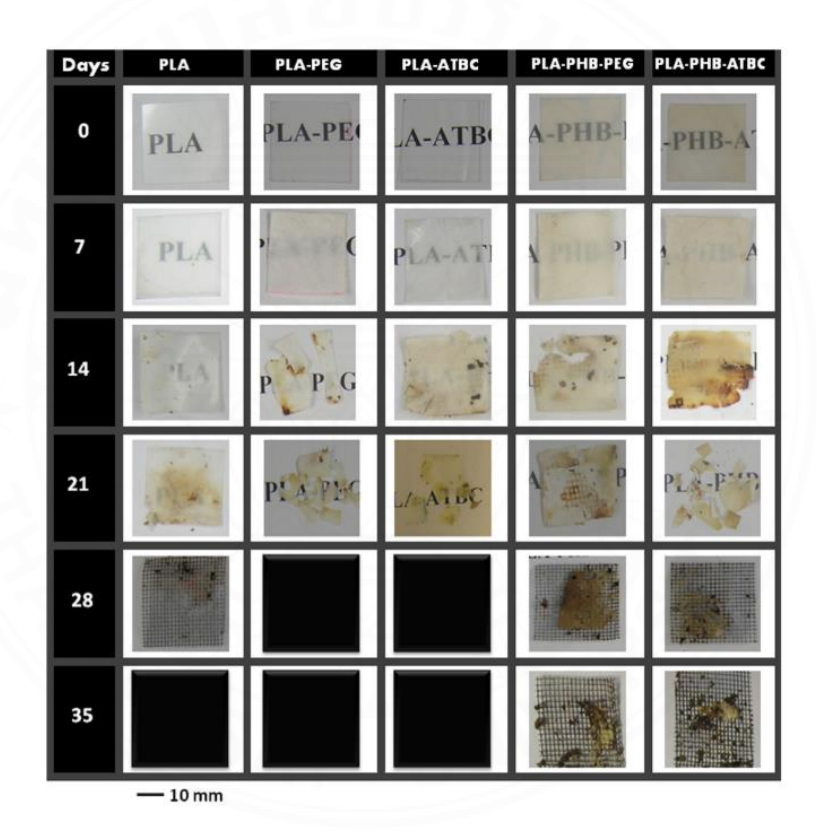


**Figure 2.3** Visual aspect of plasticized PLA and PLA-PHB films at different disintegration times. (Arrieta et al., 2014)

Wen et al. successfully prepared nanocomposite films from poly(vinyl alcohol) (PVA) with zinc oxide-coated multi-walled carbon nanotubes (MWCNTs-ZnO) for packaging applications. The PVA nanocomposite films exhibited enhanced properties over pure PVA, including improved tensile strength, thermal stability, reduced water vapor transmission, increased hydrophobicity, and enhanced antibacterial activity.

Notably, water loss tests on vegetables stored at room temperature demonstrated that those wrapped in PVA nanocomposite films containing 0.6% MWCNTs-ZnO (0.6(MWCNTs-ZnO)/PVA) retained a higher moisture content for up to 4 days. The result showed a low rate of water loss in vegetables when packed in PVA nanocomposite films. This results in the vegetables maintaining a higher level of freshness compared to those packed with pure PVA or without any packaging film, as seen in Figure 2.4.

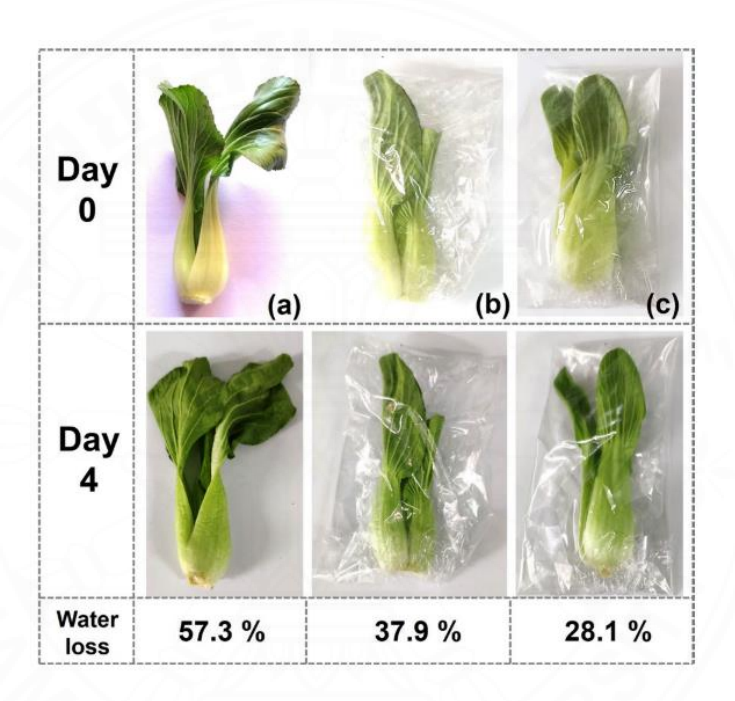


**Figure 2.4** Vegetable rate of water loss a) control, b) PVA and c) 0.6(MWCNTs-ZnO)/PVA. (Wen et al., 2022)

He et al. have recently successfully prepared antimicrobial films by combining lignin and cellulose with polylysine (PL). The films were made with a lignin content of 30% and a polylysine concentration of 3% (LRCPL30-3). The films exhibited excellent antibacterial, hydrophobicity, water vapor, and oxygen barrier properties and high tensile strength. Based on these results, the LRCPL30-3 material was utilized for shrimp packaging, significantly extending the product's shelf-life, as illustrated in Figure 2.5.



**Figure 2.5** Multifunctional cellulose-lignin films (LRCPL30-3) applied as packaging materials for shrimp. (He et al., 2023)

#### 2.2 Poly(lactic acid) (PLA)

The increasing focus on sustainability, environmental consciousness, and government policy is motivating both industries and researchers to research and develop bio-based and biodegradable products. (Lu et al., 2014). PLA, or poly(lactic acid), stands out as a widely utilized biodegradable aliphatic polyester for its similarity to petrochemical polymers. It is derived from 1- and d-lactic acid from the fermentation of starch-rich plants like corn, sugar cane, cassava, bagasse, wood chips, and wheat straw (Angin et al., 2022; Fortunati et al., 2012; Kumar et al., 2019).

Figure 2.6 Synthesis of poly(lactic acid). (Xiao et al., 2012)

PLA is synthesized either by the direct polycondensation of lactic acid monomers or through the ring-opening polymerization of lactide. Since lactic acid exists in two isomeric forms, L- and D-lactic acid, three distinct stereochemical variations of lactide are possible: L,L-lactide, D,D-lactide, and L,D-lactide. These stereochemical configurations significantly influence the final properties of PLA (Peelman et al., 2013).

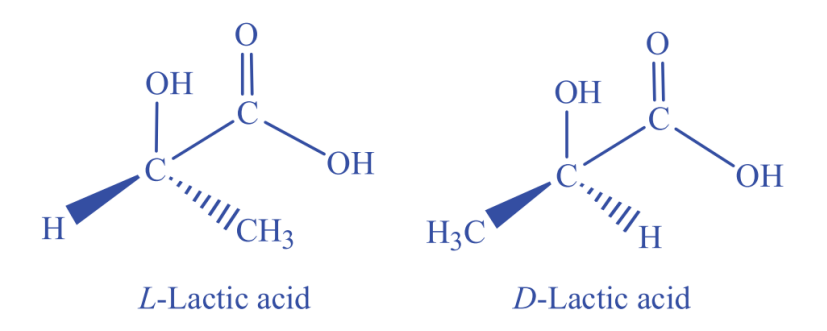


Figure 2.7 Isomers of lactic acid. (Xiao et al., 2012)

The standout properties of PLA are its eco-friendliness, high tensile strength, stiffness, and biodegradability. On the other hand, it has brittleness, poor mechanical performance, and limited barrier properties. These constraints restrict its usage in packaging. One method to enhance PLA's properties is mixing other polymers, plasticizers, or fillers like starch, carbon, and cellulose fibers into the PLA matrix, thereby improving its overall characteristics. (Kumar et al., 2019; Paul et al., 2021; Popa et al., 2017).

Many studies have been conducted to address the limitations of biopolymers, which include relatively low tensile strength, poor flexibility, and barrier properties, hindering their industrial utilization. These biopolymers, despite their eco-friendly degradation characteristics, require enhancements to meet broader industrial demands. One approach involves incorporating reinforcing agents like nanofillers, biopolymers, plasticizers, and natural additives to augment their mechanical and functional properties, thereby expanding their applicability while maintaining their environmentally friendly disposal traits (Kumari et al., 2022; Perera et al., 2023).

#### 2.3 PLA bio-composites

PLA bio-composites represent a significant advancement in sustainable materials research, integrating the advantages of PLA with various natural fibers or fillers. PLA, a biodegradable polymer from renewable materials such as corn starch or sugarcane, is distinguished for its eco-friendly characteristics. Nevertheless, its mechanical properties and uses can be significantly improved when combined with natural fibers such as hemp, flax, or bamboo. Incorporating natural fibers with PLA produces a bio-composite that reduces dependence on petroleum-derived polymers

while enhancing the material's strength and durability. These bio-composites are lighter and can be modified for specific uses, making them suitable for automotive components, packaging, and construction materials (Mohanty et al., 2000; Sudamrao Getme & Patel, 2020).

The PLA bio-composite can enhance PLA's mechanical, thermal, and gas barrier properties. Many research investigations focus on enhancing the toughness, strength, and water vapor permeability (WVP) of polylactic acid (PLA), focusing on improving the compatibility between the PLA matrix and fillers by using various methods listed in Table 2.1. For instance, Guo et al. successfully developed PLA/clay nanocomposite (PLA-30B) utilizing the melt-blending process. The results indicate that adding clay at 1 phr to the PLA-30B yields a high elongation at break of 208%, corresponding to the morphological investigation showing the clay is well-dispersed within the PLA matrix. Jaikaew et al. successfully researched PLA/silica bio-composite films. This research involves modified silica with poly(lactic acid-grafted-chitosan) copolymer (PCT). The PLA/silica bio-composite films were prepared using a compression molding technique. The resulting results indicate that the PLA/silica biocomposite films exhibit the greatest reduction in light transmission at the addition of 5 %wt. silica (Jaikaew et al., 2018). Wang et al. studied the PLA/wheat starch biocomposite blended with methylenediphenyl diisocyanate (MDI) using melt blending. The PLA bio-composite, including 45% wheat starch and 0.5 %wt MDI, has a maximum tensile strength of 68 MPa and an elongation at break of 5.1% (Wang et al., 2002). Kale et al. successfully manufactured PLA/MCC derived from rice bran oil using the solvent casting method. MCC was modified by resultant acylated MCC (RAMCC) to enhance hydrophobicity. The mechanical, thermal, and UV barrier properties of PLA/RAMCC exhibit excellent characteristics. The WVP decreased upon the addition of 2 %wt RAMCC (Kale et al., 2018). The characteristics of PLA biocomposites are based on the filler utilized. The mechanical and gas barrier characteristics were greatly enhanced by the filler in the PLA matrix processing methods. The difference in these composite properties. However, this was determined by the filler and methods (Sudamrao Getme & Patel, 2020). Kumar et al. effectively developed nanocomposite films of PLA with cellulose nanofibers (PLA/CNFs) using solvent casting methods. The PLA/CNFs film demonstrates exceptional mechanical and barrier properties upon incorporating 5 wt% CNFs into the PLA matrix. Yu et al. successfully produced a composite filament of PLA with rice straw powder (RSP) with fused deposition modeling (FDM) 3D printing. The PLA composite filament displays enhanced tensile strength and modulus upon the incorporation of RSP after alkaline and ultrasonic pretreatment (Yu et al., 2021).



 Table 2.1 Mechanical and gas barrier properties of PLA bio-composite

			Mechanical properties					
Polymer/Filler	Modification	content	Processing method	Tensile strength (MPa)	Young's modulus (MPa)	Elongation at break (%)	Gas barrier properties	Reference
PLA/clay	- /	1 phr	Melt blending	$50.8 \pm 0.8$	$1,640 \pm 70$	$208 \pm 45$	-	(Lai et al., 2014)
PLA/silica	PCT	5 %wt.	Compression molding	<u> </u>		-/11/-	High WV	(Jaikaew et al., 2018)
PLA/starch	MDI	45 %wt.	Melt blending	68.06	1,810	5.1	-	(Wang et al., 2002)
PLA/MCC	Acylation	2 %wt.	Solvent casting	36.66	424	8.8	Low WVP	(Kale et al., 2018)
PLA/CNFs	-	5 %wt.	Solvent casting	35.61		-	Low WVTR	(Kumar et al., 2019)
PLA/RSP	-	1:99	3D printing	58.59	568.68	-	-	(Yu et al., 2021)

#### 2.4 Cellulose

Due to their full biodegradability, nontoxicity, and low density, natural fibers have immense potential for reinforcing thermoplastic matrixes. Cellulose is the most commonly utilized natural polymer, produced by plants such as wood pulp, rice husk, sugarcane bagasse, cotton linter, and banana, as well as by bacteria, through a process known as delignification (Mohamed et al., 2017; Peelman et al., 2013; Spiridon et al., 2016). Cellulose, the most abundant polysaccharide in nature, is the primary structural component of all plant fibers. It is an organic polymer with the formula (C<sub>6</sub>H<sub>10</sub>O<sub>5</sub>)<sub>n</sub>, composed of linear chains of  $\beta$ -(1 $\rightarrow$ 4) linked D-glucose units, which can range in length from several hundred to several thousand units. The degree of polymerization varies depending on the source, with values reaching up to 14,000 g/mol. As a major constituent of dietary fiber, cellulose forms tightly packed linear molecules that create long, insoluble fibers, making it resistant to digestion by human enzymes. It is also a crucial structural element in the cell walls of green plants and algae, contributing to their strength and structure. The cellulose matrix exhibits extensive intermolecular hydrogen bonding, which aligns the molecules in a parallel orientation, leading to the formation of microfibrils. This structure consists of a crystalline phase interspersed with an amorphous phase, with the ratio between them varying based on plant species and structural organization (Collard & Blin, 2014; Mudgil & Barak, 2013).

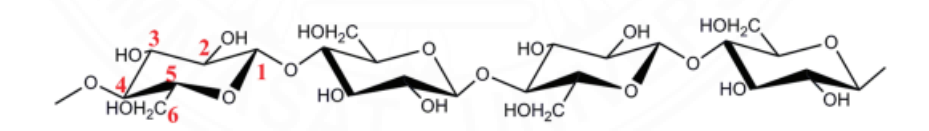


Figure 2.8 Structure of cellulose. (Zhang et al., 2011)

Various techniques have been employed to extract cellulose and analyze the chemical composition of plant fibers, including cellulose, lignin, and hemicellulose, as shown in Table 2.2. Sheltami et al. successfully isolated cellulose and cellulose nanocrystals from mengkuang leaves (Pandanus tectorius) using alkali treatment and bleaching, with cellulose extracted by treating the leaves with a 4% NaOH solution at 125 °C. The isolated cellulose was then bleached using a 1.7% NaClO<sub>2</sub> solution at 125 °C for 4 h. The cellulose nanocrystals were obtained through acid hydrolysis of

cellulose using 60 %wt. H<sub>2</sub>SO<sub>4</sub> at 45 °C for 45 min and then sonicated for 30 min. The cellulose has sizes ranging 5 - 80 µm, while the cellulose nanocrystals have dimensions ranging 5 - 25 nm. The cellulose structures were examined using FTIR spectroscopy and X-ray diffraction (XRD). The analysis reveals that hemicellulose and lignin were effectively extracted from the isolated cellulose (Sheltami et al., 2012). Nuruddin et al. produced cellulose nanofibers (CNFs) from kenaf fibers and wheat straw using a method that involved treatment with formic acid (FA)/acetic acid (AA), peroxyformic acid (PEA)/peroxyacetic acid (PAA), and hydrogen peroxide (H<sub>2</sub>O<sub>2</sub>), followed by ball milling. The CNFs were analyzed using FTIR spectroscopy, SEM microscopy, Transmission electron microscopy (TEM), XRD, and thermogravimetric analysis (TGA). The ball milling process successfully extracted CNFs with diameters ranging from 8 to 100 nm. The preparation of CNFs mostly removed lignin and hemicellulose from lignocellulose, resulting in an enhanced crystallinity. Moreover, the decomposition temperature of CNFs increased by about 27 °C (Nuruddin et al., 2015). Different treatment techniques for cellulose fiber can yield a variety of micro- and nanosized cellulose fiber products. These methods generate cellulose fibers presenting distinct crystallinities, fiber dimensions, and functionalities (Jiang & Ngai, 2022).

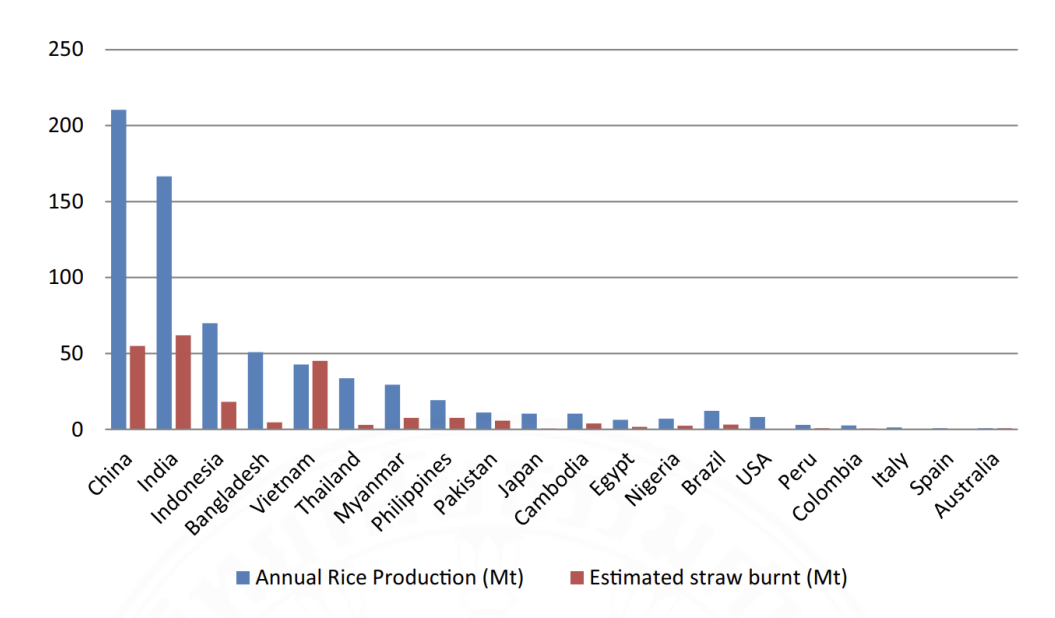
Cellulose is a popular material for polymer composites due to its low production cost and ability to produce high-performance products. Cellulose is inexpensive, compatible with living organisms, and biodegradable from numerous renewable sources. Cellulose possesses several beneficial properties, such as remarkable strength and stiffness, and contains numerous hydroxyl groups amenable to modification through different chemical processes. Despite its considerable potential as a biological reinforcement in bio-composites, its dispersion in hydrophobic matrices is constrained by its hydrophilic nature, stemming from the high concentration of hydroxyl groups in its molecular structure. Thus, surface modification methods before being composited with the polymer can overcome this problem, and surface modification has many methods, e.g., physical and chemical treatments, which have promoted interfacial interaction between cellulose surfaces and polymer matrix (Paul et al., 2021).

Table 2.2 Extraction methods, diameter, and percentage composition of cellulose's chemical components from various natural sources.

Callulaga gaumaag	Extraction method	Diameter	Content (%weight)			Dof	
Cellulose sources	Extraction method	Diameter	cellulose	lignin	hemicellulose	Ref.	
Mengkuang leaves	Chemo-mechanical treatment	5 – 25 nm	$81.6 \pm 0.6$	$24 \pm 0.8$	$34.4 \pm 0.2$	(Sheltami et al., 2012)	
Kenaf fiber wheat straw	Chemo-mechanical treatment	8 – 100 nm	7			(Nuruddin et al., 2015)	
Sisal fiber		5 ± 1.5 nm	$62.6 \pm 2.8$	$7.9 \pm 1.0$	12.5 ± 2.5		
Hemp fiber	Chemo-mechanical treatment	20 – 50 nm	$70.6 \pm 3.6$	$4.2 \pm 0.8$	15.6 ± 2.9	(Mondragon et al., 2014)	
Flax fiber		15 – 45 nm	66.3 ± 3.5	$2.2 \pm 0.1$	$18.8 \pm 2.7$	-	
Sisal fiber	Chemical treatment	30.9 ± 12.5 nm	$\# \mathcal{F}$	765/3	_// -	(Morán et al., 2007)	
Rice straw	Chemo-mechanical treatment	70 – 90 nm	79.3	4.8	15.9	(Nasri-Nasrabadi et al., 2014)	
Rice straw	Chemical treatment	< -/IN	36.8	5.8	28.6	(Zhou et al., 2024)	
Rice husk	Chemical treatment	15 – 20 nm	96	21	12	(Johar et al., 2012)	

#### 2.5 Rice straw

Rice is a key grain and a staple food for over half of the global population, with particularly high consumption rates in growing economies and Asian countries. It represents approximately 95% of global production and is consumed by around 50% of people worldwide. In terms of agricultural commodity production, rice ranks third, following sugarcane and maize (Rathna Priya et al., 2019). Agricultural crop wastes are considered the most abundant source of cellulose owing to their worldwide abundance and yearly renewability. Rice straw (RS), a major by-product of grain crops, is often regarded as the greatest agricultural waste. Rice straw is mostly burned. It can be seen in Asia countries such as India, China, Vietnam, and Thailand, as shown in Figure 2.9 (Ramos et al., 2023). Wherewith this method is easy and low-cost. Moreover, this method can dispose of weed seeds well and reduce the presence of other diseases. On the other hand, natural waste combustion often produces considerable amounts of carbon emissions and air pollution, contributing to climate change, global warming, and PM 2.5. Due to its abundance, rice straw trash disposal has a significant effect, with much research being conducted to find helpful and practical solutions to recycle this waste. Numerous strategies for making effective use of rice straw have been devised, reducing the need for rubbish to be burnt. After treatment with chemical or physical, it's used as a fuel for animal nutrition or a natural additive in composites. Utilizing rice straw as a composite component in bio-composites can substantially minimize environmental pollution, save scarce forest and petroleum resources, and increase the added value of rice straw. Rice straw is inexpensive, biodegradable, lightweight, and has a high strength-to-weight ratio. Composites are used for natural fibers and biological waste. Natural fibers, on the other hand, have a high moisture absorption and uneven fiber diameters, which deteriorate the mechanical properties in which they are employed if not treated properly (Osman & Atia, 2018; Rathna Priya et al., 2019).



**Figure 2.9** Comparison of rice straw burning and production in each country. (Singh et al., 2021)

#### 2.6 Alkyl ketene dimer

Alkyl ketene dimer (AKD) is a fatty acid dimer synthesized from stearic acid or a blend of fatty acids with alkyl groups containing carbon chains of 16 to 18 atoms, along with a single lactone ring, as shown in Figure 2.5. The melting point of AKD varies between 40 and 60 °C, depending on the length of the carbon chain in the dimer (Quan et al., 2009). AKD is classified as waxy and emulsion. Another study indicates that liquids are less effective as a sizing agent than wax (Hundhausen et al., 2008). The AKD emulsion is prepared by dispersing particles in an aqueous mixed solution, producing a milky appearance. The properties and stability of the emulsion improve with increasing AKD oligomer concentration, and the particle size of the AKD emulsion ranges from 0.2 to 2 μm (Kumar et al., 2016).

Figure 2.10 Structure of alkyl ketene dimer (AKD). (Hundhausen et al., 2008)

AKD highly reacts to chemical reactions with hydroxyl groups (-OH groups), especially cellulose (Ali Varshoei, 2013). The interaction between the lactone ring of AKD and the hydroxyl groups of cellulose creates a  $\beta$ -ketoester bond on the cellulose surface, with the hydrophobic tails aligning as side chains, enhancing its hydrophobic characteristics. Furthermore, AKD is commonly used as an affordable, food-safe neutral sizing agent in the paper industry, where its high hydrophobicity improves the water resistance of paper (Kaewsaneha et al., 2022).

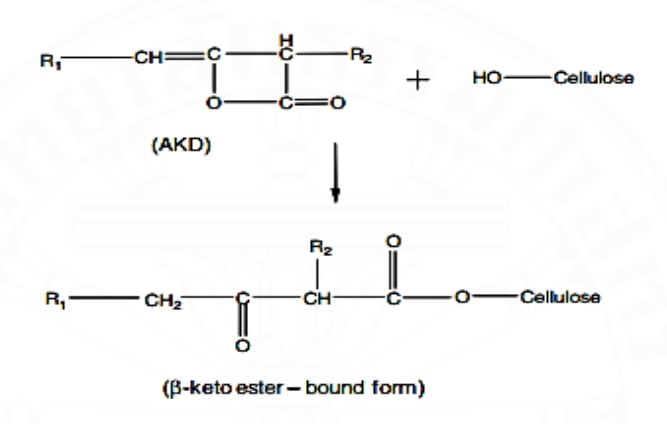
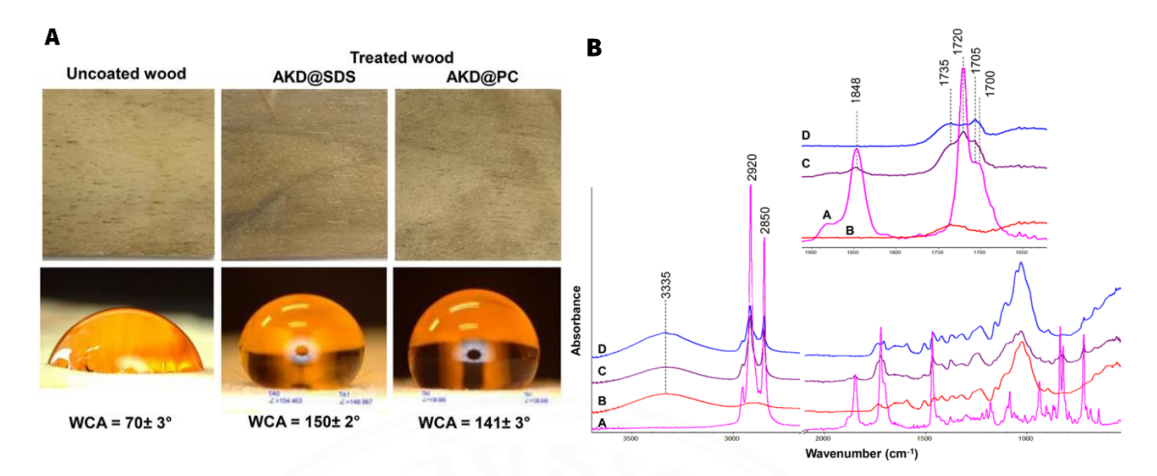


Figure 2.11 Reaction of cellulose treated with AKD. (Kumar et al., 2016)

Several researchers have focused on the surface modification of cellulose by using AKD to develop hydrophobicity. Kaewsaneha et al. effectively prepared wood treated with AKD nanoparticles by subjecting it to heating at 110°C for 5 hours. Figure 2.12 presents the water contact angle and FTIR spectra of wood treated with AKD. The treated wood shows a water contact angle (WCA) of  $150^{\circ} \pm 2$ , indicating the presence of a hydrophobic layer on the surface. FTIR analysis reveals the reaction between the lactone ring of AKD and the wood's hydroxyl groups, with a new peak at 1735 cm<sup>-1</sup> confirming the formation of a  $\beta$ -ketoester bond.



**Figure 2.12** water contact angle of treated wood and FTIR spectra of neat AKD (A), untreated teakwood (B), and teakwood samples treated with AKD@SDS (C) and AKD@PC (D). (Kaewsaneha et al., 2022)

Yang et al. successfully produced alkali/urea regenerated cellulose (AUC) films treated with AKD, resulting in AUC-AKD films. The film has a maximum content of AKD at 0.2%. The AUC-AKD films exhibit a significant increase in WCA from 50 to 110 degrees following treatment with AKD. The water vapor permeability (WVP) of AUC-AKD is lower than AUC films at the same relative humidity (RH). However, when relative humidity (RH) increases, the WVP of AUC-AKD films also increases as seen in Figure 2.13.

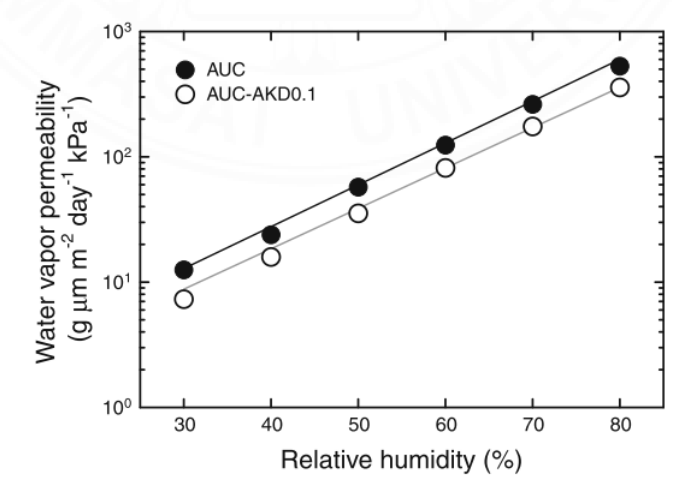


**Figure 2.13** Effect of relative humidity on water vapor permeability of AUC and AUC–AKD0.1 films. (Yang et al., 2012)

Caylak et al. successfully investigated the impact of AKD on PLA composite films containing natural fiber (NF) and glass fiber (GF). A twin-screw extruder was used to produce PLA composite film using melt-compounding. The mechanical characteristics of PLA composite films demonstrate a 40% improvement in mechanical strength compared to PLA composite films without AKD. The WCA of PLA composite films is greater when AKD is present compared to PLA composite films without AKD. Furthermore, AKD enhances the compatibility between PLA and NF/GF, as shown in Figure 2.14. This is attributed to the well-dispersed NF with AKD in the PLA matrix, which results in improved mechanical characteristics. This improvement can be attributed to enhanced interfacial interaction between PLA and NF/GF.

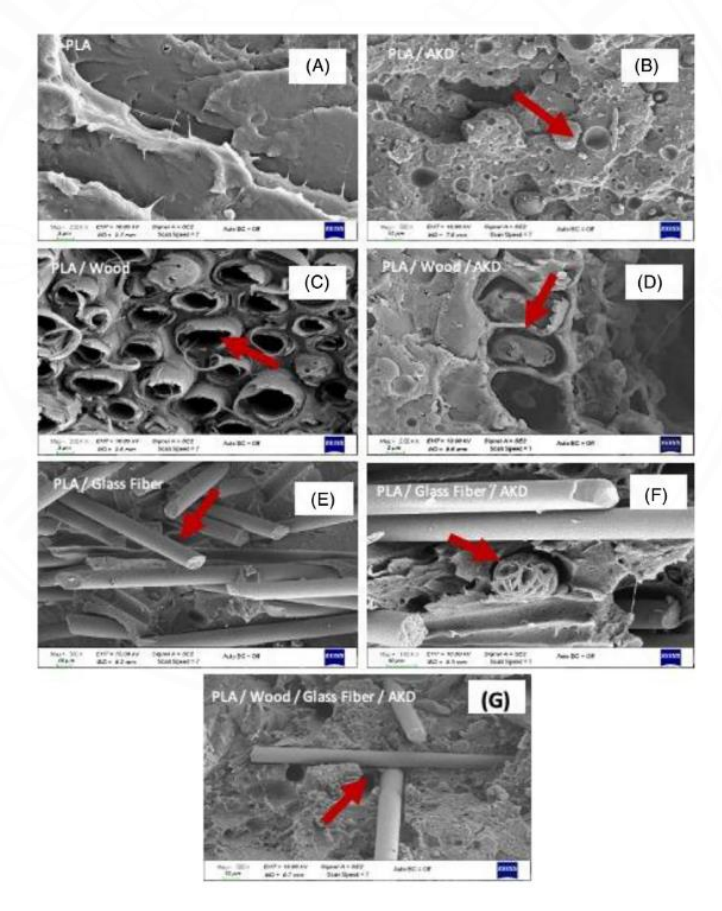


**Figure 2.14** SEM images of the fractured surface of the composites: (a), neat PLA; (B), PLA with AKD; (C), NF-filled PLA; (D), NF-filled PLA with AKD; (E), GF filled PLA; (F), GF filed PLA with AKD; (G), NF and GF filled PLA with AKD. AKD, alkyl ketene dimer; PLA, poly(lactic acid). (Caylak et al., 2021)

#### 2.7 Ball milling

Ball milling is a widely used technique for breaking down particles and reducing their size. During this process, powder particles are trapped between colliding balls and the inner surface of the milling container. This leads to repeated deformation and breakdown of the powder, resulting in the production of fine nanoparticles (Piras et al., 2019). This technique offers several benefits, including cost-effectiveness, reliability, ease of use, and the ability to generate consistent results through control of energy and speed. It can be applied in both wet and dry conditions and is compatible with various materials, such as cellulose, chemicals, fibers, polymers, hydroxyapatite, and metal oxides. One notable application in the field of cellulose is the preparation and chemical modification of cellulose nanocrystals and nanofibers. This approach allows for the integration of chemical treatments, facilitating the production of desired products with minimal effort. However, factors such as milling duration, processing speed, solvent choice, and pre-treatment methods need to be carefully optimized, as they can significantly impact the properties of the isolated nanocellulose. This allows for precise manipulation of the final particle size and distribution.

By adjusting these parameters, it is possible to tailor the milling process to meet specific requirements, such as achieving submicron or nanoscale particles. As well-known, esterification is the most frequently documented reaction on the functionalization of CNCs and CNFs as shown in Figure 2.15. The chemical reactivity of these materials is often challenging due to their limited solubility in both water and organic solvents. However, it is possible to investigate alternative forms of chemical modification, although this is restricted by the functional groups that are present. Other potential reactions could involve the cellulose hydroxyl groups acting as nucleophiles. Additionally, the adaptability of ball milling in dry and aqueous environments positions it as a promising, environmentally friendly, and sustainable technology for industrial use. Further investigation into the synthesis of cellulose-based nanocomposites is recommended, as this method provides a straightforward and efficient approach for creating these hybrid systems. Some studies have been proposed on developing modification and extraction of cellulose fiber. For example, Lan et al. studied pretreated microcrystalline cellulose (MCC) to enhance its performance in photoreforming using

a Pt/TiO<sub>2</sub> catalyst. The findings show that the ball milling treatment could significantly modify the MCC with decreased particle size and improved photoreforming of MCC for H<sub>2</sub> production (Lan et al., 2022). Nuruddin et al. developed a method for extracting cellulose nanofibers from lignocellulosic biomass through ball milling and chemical treatment. Their study showed significant removal of lignin and hemicellulose from kenaf fiber and wheat straw, while preserving the original cellulose structure of the isolated nanofibers. There are obtained a cellulose nanofiber with a uniform diameter ranging from 8 to 100 nm (Nuruddin et al., 2016). Huang et al. conducted a study on modifying cellulose nanofibers to enhance their dispersion in an organic solvent. The researchers employed the ball milling method to modify native cellulose using hexanoyl chloride as an esterifying agent through wet mechanical ball milling. By varying the milling duration, they examined its effects on the modification process. The results showed a progressive increase in the ester bond peak in the FTIR spectrum with longer milling times. Furthermore, stability tests demonstrated a well-dispersed state, consistent with the FTIR findings (Huang et al., 2012).

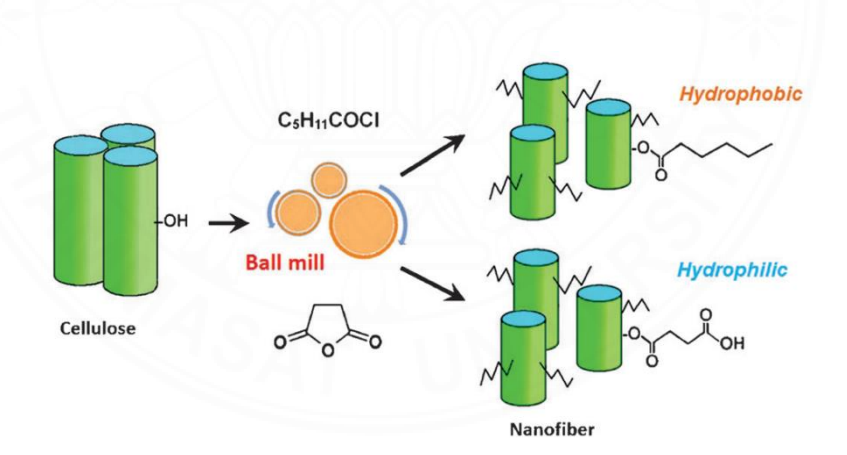


**Figure 2.15** The modification of surface cellulose nanofibers with esterification through ball milling (Huang et al., 2012).

#### **CHAPTER 3**

#### EXPERIMENTAL APPROACH

The overall process for PLA/modified cellulose bio-composites preparation is summarized in Figure 3.1. The preparation of PLA/RSC cellulose bio-composites is divided into 3 parts. In the first part, rice straw cellulose fiber (RSC) was extracted from rice straw (RS) by a chemical treatment (alkaline, bleaching, and acidic treatments) (Fig 3.1a). In the next step, the surface of cellulose fiber is modified by grafting alkyl ketene dimer (AKD) on hydroxyl group (-OH) cellulose using ball-milling machine, subsequently by treatment in a hot-fan oven to allow a ring-opening reaction of lactone ring of AKD by reacted with hydroxyl group (-OH) of cellulose forming β-ketoester bond at 110 °C (Fig 3.1b). Lastly, the modified particles/fibers are further used as reinforcing fillers for commercial Poly(lactic acid) (PLA). The films were prepared using the solvent-casting method (Fig 3.1c). The chemical structure of the extracted products and the interaction between cellulose and AKD were studied using Fouriertransform infrared spectroscopy (FTIR). A scanning electron microscope (SEM)was applied to observe the morphology and determine the particle size of modified products. Hydrophobicity, mechanical properties, and water vapor permeability (WVP) of the PLA/modified cellulose bio-composites were investigated.

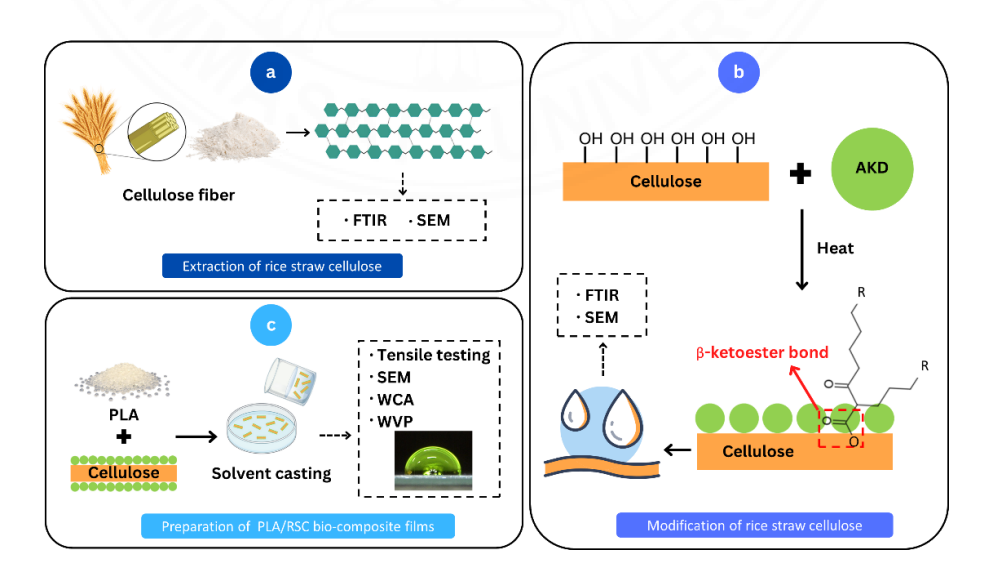


**Figure 3.1** The overall process of (a) extraction of RSC, (b) RSC surface modification, and 1(c) fabrication of PLA/RSC bio-composite films.

#### 3.1 Materials

Rice straw (RS) was supplied by a local farm in Kanchanaburi Province, Thailand. Microcrystalline cellulose (MCC) was obtained from Saim Cement Group (SCG). Poly (lactic acid) (PLA) pellets (Ingeo<sup>TM</sup> Grade 4043D) was purchased from NatureWorksLLC. Sodium hydroxide (NaOH) pellets, Hydrogen peroxide (H<sub>2</sub>O<sub>2</sub>) 40%, Hydrochloric acid (HCl) 37%, and Tetrahydrofuran (THF) were purchased from Carlo Erba<sup>TM</sup>. Alkyl Ketene Dimer (C16-C18 grade) was purchased from Kemira Co. Ltd. Chloroform 99.8% from RCI Labscan<sup>®</sup>.

#### 3.2 Experimental

#### Part I Extraction and characterization of rice straw cellulose (RSC)

#### 3.2.1 Extraction of RSC

The Rice straw Cellulose fibers (RSC) extraction process was adopted from Nasri-Nasrabadi et al. (2014) method. The overall extraction process includes alkaline treatment, bleaching, and acidic treatment. Rice straw was initially washed and dried in a vacuum oven at 80 °C for 24 h. Then, 10 g of rice straw was immersed and stirred in a NaOH solution (4 *%wt*.) at 60 °C for 4 h. The bleaching procedure was then subsequently performed by adding the obtained alkaline treated cellulose fibers into H<sub>2</sub>O<sub>2</sub> solution (10 *%v/v*.) at 80 °C for 2 h. In the final step, the acidic treatment was conducted in an HCl solution (10 *%v/v*.) at 60 °C for 12 h. A dialysis process was applied to neutralize the cellulose fiber products. The obtained RSC was dried in an oven at 80 °C for 24 h. The procedure for the extraction process is shown in Figure 3.2.

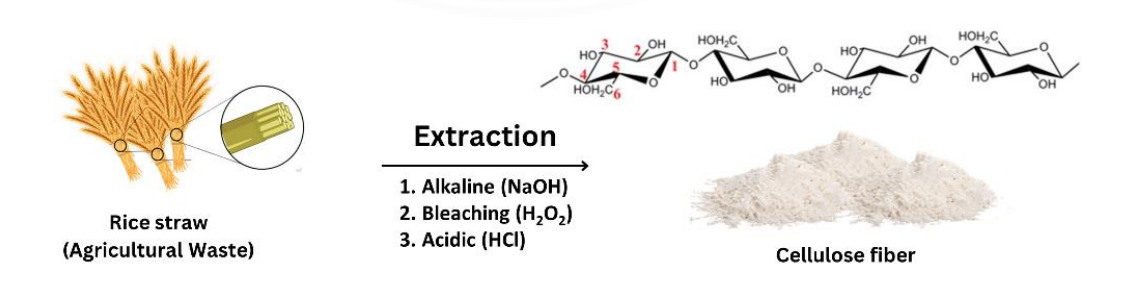


Figure 3.2 The procedure for the extraction process

#### 3.2.2 Characterization of RSC

The yield of RSC was determined using equation 3.1, yield (%):

$$Yield (\%) = \frac{Wfinal}{Wstarting} \times 100$$
 (3.1)

Where: W<sub>final</sub> is the weight of RSC after acidic treatment

W<sub>starting</sub> is the weight of RS.

The FTIR spectra of RSC and its modified fibers/particles were recorded on a Fourier-transform infrared (FTIR) spectroscopy (Nicolet iS5 spectrometer) in an attenuated total reflection (ATR) mode. The spectra were collected using 32 scans and a resolution of 4 cm<sup>-1</sup>.

Field Emission Scanning electron microscope (JSM-6000 Plus, JEOL) and image J Software were used to observe morphology and determine the size of RSC and modified RSC, respectively. The voltage of 2 kV, with 500X and 5000X are applied. The dried samples were dispersed on a stub's carbon tape before gold coating.

# Part II Preparation of RSC treated with AKD (RSCD)

# 3.2.3 Conditions screening for surface modification of cellulose using AKD.

Commercial microcrystalline cellulose (MCC), which has a chemical structure similar to RSC, was used in the screening step to determine the best treatment conditions for AKD-treated RSC. The MCC was treated with AKD in a ball-milling machine (Planetary ball mills (PM100, Retsch) at a speed of 500 rpm for 1 h. The reaction of AKD and hydroxyl group (-OH) of cellulose was further employed in an oven at 110 °C (Kaewsaneha et al., 2022). The reaction time was varied at 1, 2, 3, 4, 5, and 15 h, and the content of AKD was fixed at 10 *%wt*. The best operating conditions will be further used for the AKD treatment RSC in the next step.

#### 3.2.4 Modification of RSCD

The RSC was then treated with AKD in a ball-milling machine at a speed of 500 rpm for 1 h. The content of AKD was fixed at 10 %wt. of RSC. The surface-treated RSCD was subsequently heated in an oven at 110 °C for 15 h. The RSCD was washed in THF and dried in a vacuum oven at 60°C overnight. The chemical reaction among AKD and the hydroxyl groups (-OH) of RSC was studied and confirmed by FTIR. The surface morphology and particle size of RSCD were examined by SEM at 500X, 1000X, and 2000X resolution and image-j software. The chemical reaction of the AKD-treated RSC is shown in Figure 3.3.

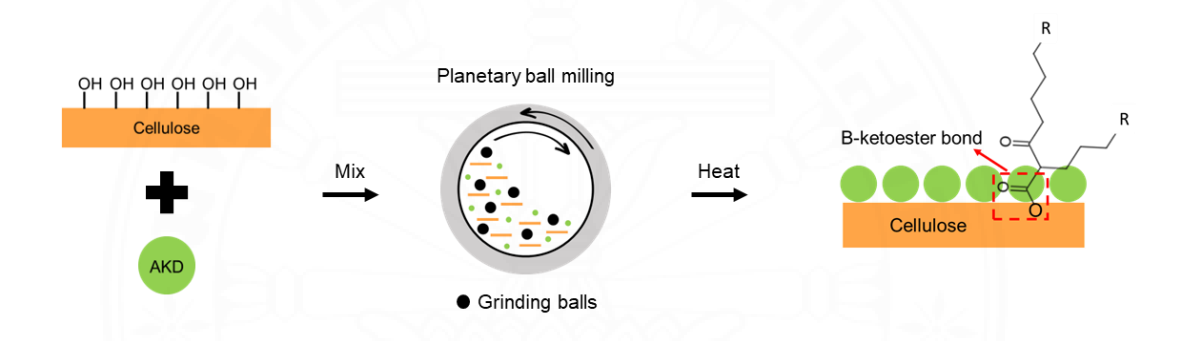


**Figure 3.3** The overall procedure for the AKD-treated RSC and their characterization.

# <u>Part III</u> Fabrication and characterization of PLA/RSC bio-composite films 3.2.5 Fabrication of PLA/RSC bio-composite films

Neat PLA and PLA/RSC bio-composite films were prepared using a solvent-casting method. RSC was dissolved and dispersed in PLA solution (chloroform 10 %w/v.), and the RSC contents were varied at 1, 3, 5, and 7 %wt. The mixture was then cast on a Teflon sheet and placed in a fumed hood to allow solvent evaporation for 24 h. The obtained films were then dried in a vacuum oven at 50 °C for 24 h.

## 3.2.6 Characterization of PLA/RSC bio-composite films

The chemical structure and compositions of neat PLA and PLA/RSC biocomposite films were determined by FTIR spectroscopy as described above. The neat PLA and PLA/RSC bio-composite films were cut with dimensions of  $15 \text{ mm} \times 100 \text{ mm}$  for tensile testing by using a universal testing machine following the ASTM D882.

The test was conducted at room temperature on a Tinius Olsen THE 1000N universal testing machine with a speed of 50 mm/min, a 1000 N load cell, and a 50 mm initial gauge length. Each sample was examined at least 8 times.

The morphology on the cross-section of fractured neat PLA and PLA/RSC biocomposite films from the tensile testing was observed using SEM with 700X and 1500X resolution and 2kV of voltage. The water contact angle (WCA) was measured to determine the hydrophobicity or water wettability of the material's surface using a Digital microscope (Dino-lite). The contact angle was measured using a digital microscope and a 20  $\mu$ L droplet of distilled water.

The water vapor permeability (WVP) of neat PLA and PLA/RSC bio-composite films was investigated using Mocon: PERMATRAN-W® Model 398 under condition test 90%RH, 37.8 °C.

#### **CHAPTER 4**

# **RESULTS AND DISCUSSION**

#### Part I Extraction and characterization of rice straw cellulose (RSC)

Cellulose fibers were extracted from rice straw (RS) using 3-step treatments, i.e., alkaline, bleaching, and acidic treatments. The final product is in the form of white powder and the calculated yield of the Rice straw cellulose (RSC) is around 25.2  $\pm$ 0.5% is obtained. The chemical structure and morphology of the extracted cellulose fibers were characterized using FTIR and SEM, respectively. FTIR spectrum of extracted RSC and its chemical structure is shown in Figure 4.1. The peak at 3335 cm<sup>-1</sup> <sup>1</sup> corresponds to Hydroxxyl (-OH) groups of cellulose (Chirayil et al., 2014; Nasri-Nasrabadi et al., 2014). The peak at 2895 cm<sup>-1</sup> was observed with C-H stretching vibrations of cellulose (Hozman-Manrique et al., 2023). The band at 1645 cm<sup>-1</sup> represents the -OH bending vibrations of adsorbed water (Mohamad Haafiz et al., 2013). The peak at 1317 cm<sup>-1</sup> was attributed to cellulose C-C and C-O skeletal vibrations. The absorption band at 1160 cm<sup>-1</sup> corresponds to cellulose C-O antisymmetric bridge stretching. The band at 1054 cm<sup>-1</sup> related to C-O-C skeletal vibration of the pyranose rings in cellulose. The peak at 898 cm<sup>-1</sup> was assigned to the 1,4  $\beta$ -glycosidic linkages (Chen et al., 2013; Ng et al., 2015; Reddy et al., 2015). Moreover, two peaks at 2917 and 2850 cm<sup>-1</sup> correspond to CH stretching of lignin and hemicellulose, which are not found in the spectrum. The small peak in 1729 and 1513 cm<sup>-1</sup> is associated with the carbonyl group (C=O) and C=C stretching vibration of hemicellulose and lignin (Hozman-Manrique et al., 2023; Lu & Hsieh, 2012) also not detected. The absence of these four peaks in the spectrum indicates that lignin and hemicellulose were effectively removed during the treatment process.

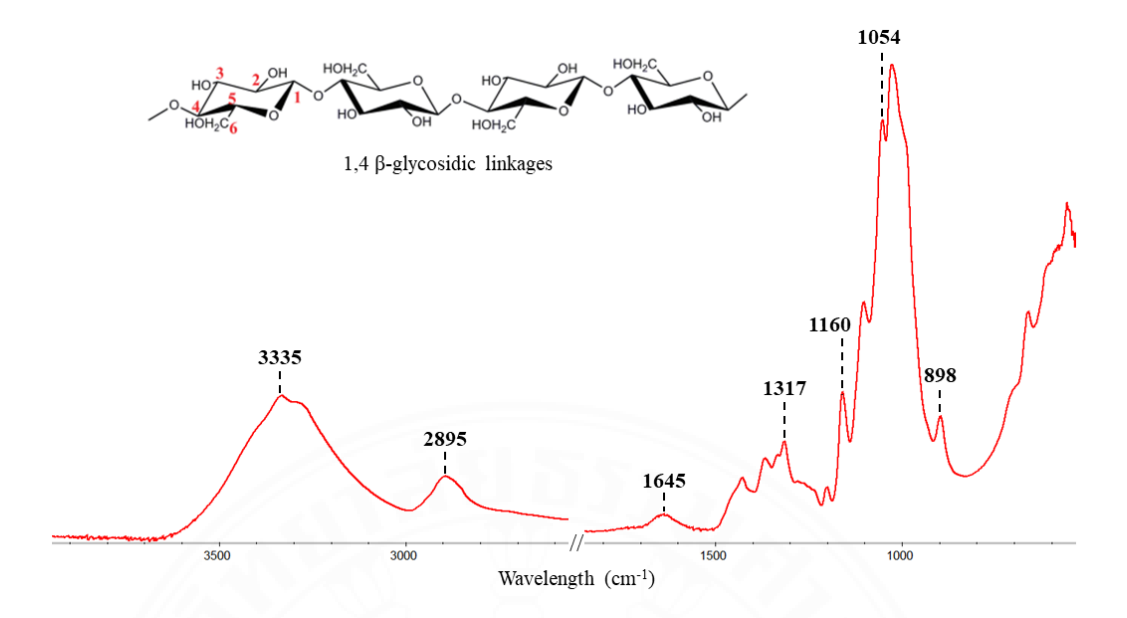


**Figure 4.1** FTIR spectrum of extracted RSC.

The morphology and size of cellulose before and after each step treatments, i.e. (1) Alkaline (2) bleaching, and (3) acid treatments, are compared and shown in Figure 4.2. The SEM image of the rice straw is shown in Figure 4.2 (a, b). A rough surface of non-cellulose components such as lignin, hemicelluloses, pectin, wax, and other impurities are observed on the fiber surface. After the first step (alkaline treatment), smaller cellulose fiber bundles are observed, and some of the non-cellulose composition and impurities are partially eliminated, as seen in Figure 4.2 (c, d). This indicates that NaOH aqueous solution can remove some cementing components on the cell wall, separating and reducing the dimension of cellulose fibers into the smaller cellulose fibers bundles. This increased surface area of the treated fibers might further increase the chance of catching up with the PLA matrix (Lu et al., 2014; Ng et al., 2015). In addition, the product from this step is light brown powder, which reflects the remaining non-cellulose components, and further treatment is required. The sample is further subject to a bleaching process using hydrogen peroxide (H<sub>2</sub>O<sub>2</sub>). The obtained product from this step is in the form of white powder. The SEM image of the bleached product is shown in Figure 4.2 (e, f). It is clearly observed that the non-cellulose component is fully removed, resulting in a clear and smooth surface. Microfibrils in the primary cell wall of fibers are believed to be removed during the bleaching process (Feng et al., 2018). However, the obtained fibers obtained from this step are presented in the form of agglomerate and large size. The acidic treatment is further applied to digest and diminish fiber size to increase the surface area of the final product. The SEM image of the fibers after acidic treatment is shown in Figure 4.2 (g, h). After acidic treatment, the fiber is in rod shape, and the diameter is reduced from  $178.2 \pm 3.1$  to  $7.4 \pm 5.4$  µm compared to the sample from the first step of alkaline treatment. The dimeter and length of fibers are reduced by separating the amorphous region from the microfibrils by an attacking of strong acid (Chirayil et al., 2014).

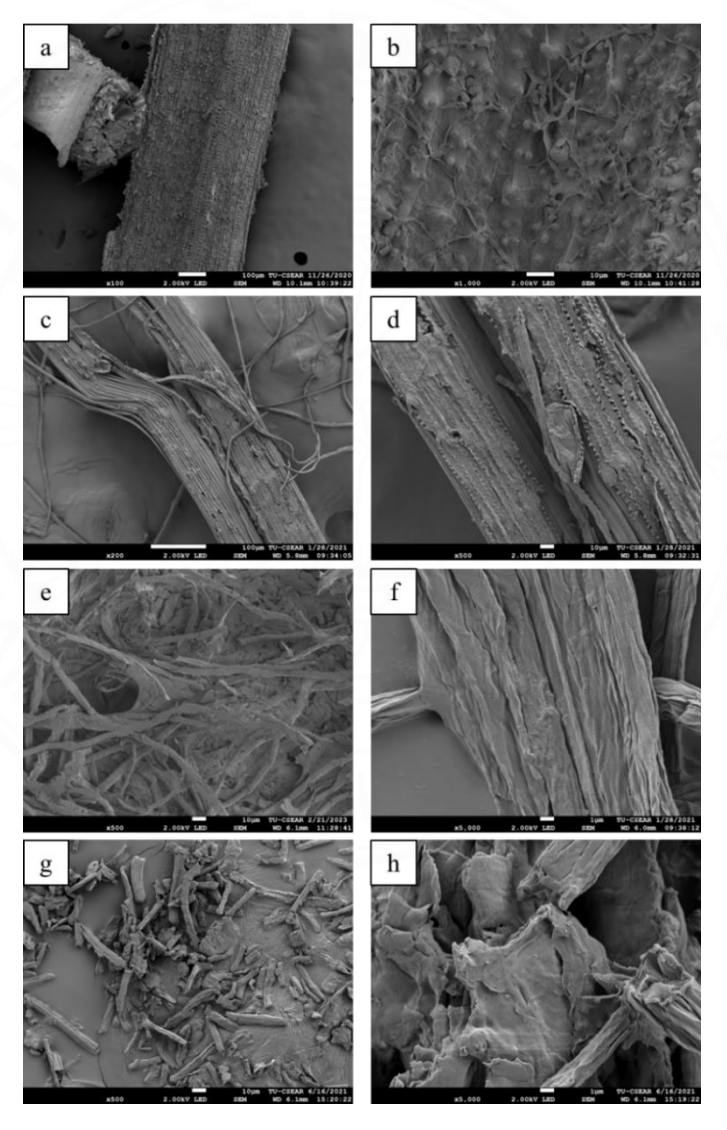


**Figure 4.2** SEM images of the extracted RS (a, b) original fiber, (c, d) alkaline treatment, (e, f) bleaching, (g, h) acidic treatment.

The chemical structures of cellulose before and after each treatment step are characterized by FTIR spectroscopy, as shown in Figure 4.3. The peak at 3335 cm<sup>-1</sup> corresponds to the OH stretching vibration of the hydroxyl group in the cellulose. The intensity of this peak increases after chemical treatment due to the removal of the noncellulose component. This key peak will be further modified and studied in this work, as it plays a crucial role in the surface moisture absorption and hydrophobicity of cellulose fibers. The presence of hydroxyl group (-OH) on the cellulose surface makes it highly reactive towards many reactions and easy to modify (Chirayil et al., 2014; Nasri-Nasrabadi et al., 2014). The native rice straw fiber shows two characteristic peaks at 2917 and 2850 cm<sup>-1</sup>, representing methylene (CH<sub>2</sub>) and methyl (CH<sub>3</sub>) stretching of lignin and hemicellulose. After the treatment process, these two peaks decreased, simultaneously with an increase of peak at 2895 cm<sup>-1</sup> of CH stretching vibrations (CH and CH<sub>2</sub>) in the cellulose fibers (Hozman-Manrique et al., 2023; Ng et al., 2015; Yan et al., 2021).

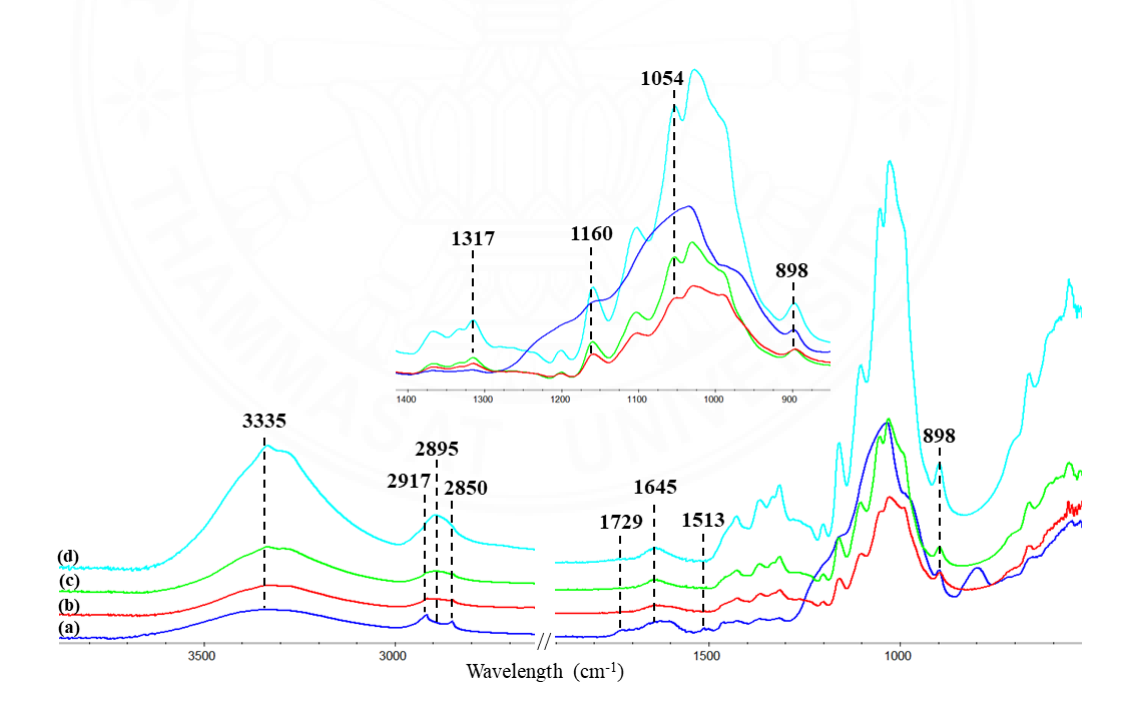


**Figure 4.3** ATR-FTIR spectra of the extracted RSC (a) original fiber, (b) alkaline treatment, (c) bleaching, and (d) acidic treatment.

In addition, the small peak at 1729 cm<sup>-1</sup> associated with the carbonyl group (C=O) from the acetyl and ester groups in hemicellulose and the ester linkages of

carboxylic groups of ferulic and p-coumaric acids in lignin is decreased after alkaline treatment and further disappeared after the bleaching process, indicating the full removal of hemicellulose and lignin (Chirayil et al., 2014; Reddy et al., 2015). The weakened and disappearance of the 1513 cm<sup>-1</sup> band, which is attributed to the C=C stretching vibration of the aromatic group in the lignin structure, are found in treated products. It is supported that lignin was completely removed after alkaline treatment (Lu & Hsieh, 2012). (Chen et al., 2013; Ng et al., 2015; Reddy et al., 2015). The results are in agreement with the SEM images discussed above. It is important to note that the absorbent band at 1645 cm<sup>-1</sup> corresponds to the absorption band of -OH bending from water molecules found in all spectra reflected a highly hydrophilic cellulose fiber (Mohamad Haafiz et al., 2013).

## Part II Preparation of RSC treated with AKD (RSCD)

Commercial microcrystalline cellulose (MCC), which has a similar chemical structure to RSC, was used in the screening step to find the best AKD treatment conditions. The FTIR spectra of MCC and RSC are compared in Figure 4.4. The band characteristics of cellulose are found at  $3335 \, \text{cm}^{-1, \, \text{which}}$  corresponds to the OH stretching vibration of the hydroxyl group in the cellulose. The CH stretching vibrations (CH and CH<sub>2</sub>) band is located at  $2895 \, \text{cm}^{-1}$  in both spectra. The band at  $1054 \, \text{cm}^{-1}$  attributed to C-O-C skeletal vibration of the pyranose rings in cellulose and peak at  $898 \, \text{cm}^{-1}$  of  $1,4 \, \beta$ -glycosidic linkages also detected in both spectra (Chen et al., 2013; Ng et al., 2015; Reddy et al., 2015). This supported the idea that the treatment process is an effective process for extracting cellulose, yielding a high-purity cellulose similar to those commercial products, which was also reported by Yan et al. (2021).

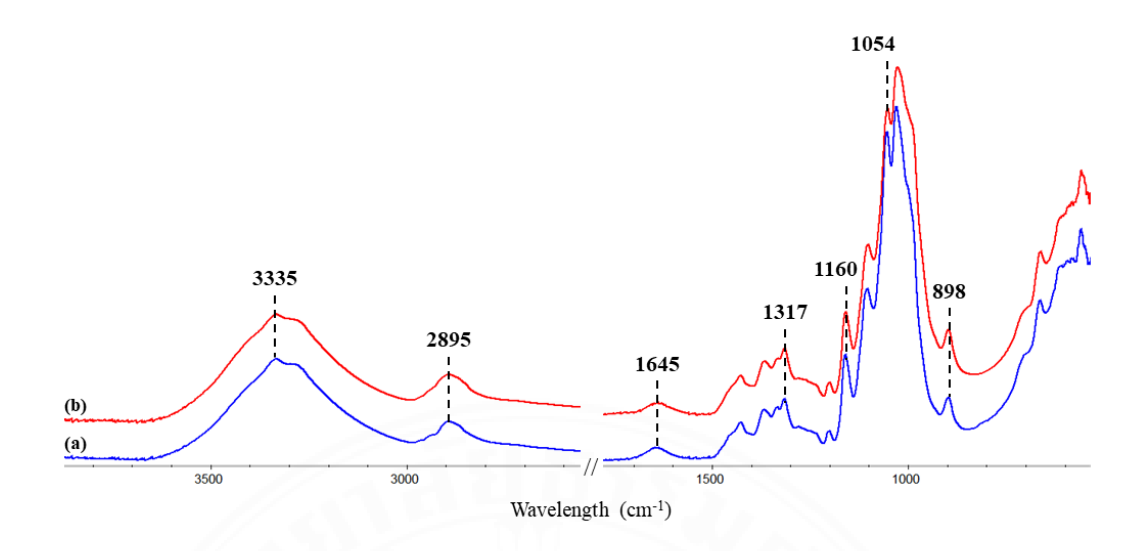


Figure 4.4 ATR-FTIR Spectrum of (a) MCC and (b) RSC.

This study uses Alkyl ketene dimer (AKD) as a modifying agent for hydroxylrich cellulose. AKD will serve as a coating agent for cellulose by disrupting H-bonds on the cellulose surface, preventing agglomeration of particles and enhancing the properties of final PLA/cellulose composite films. The chemical reaction between the lactone ring of AKD and the -OH groups of cellulose generates a β-ketoester bond on the cellulose surface, where its hydrophobic tails are arranged as hydrophobic side chains (Kaewsaneha et al., 2022). Alkyl ketene dimer (AKD) is a widely used neutral sizing agent due to its low cost, food-safe materials, and high hydrophobicity to improve the water-resistance of paper in industries. The chemical structure of neat AKD was characterized by FTIR spectroscopy, as shown in Figure 4.5. The strong bands at 2920 and 2850 cm<sup>-1</sup> correspond to the stretching vibrations of C-H in the AKD tails. In neat AKD, peaks at 1848 and 1720 cm<sup>-1</sup> are attributed to the C=O in the lactone ring and the C=C bond connected to the lactone ring, respectively. The band at 1848 cm<sup>-1</sup> will be further utilized to confirm the successful grafting of AKD onto the cellulose surface.

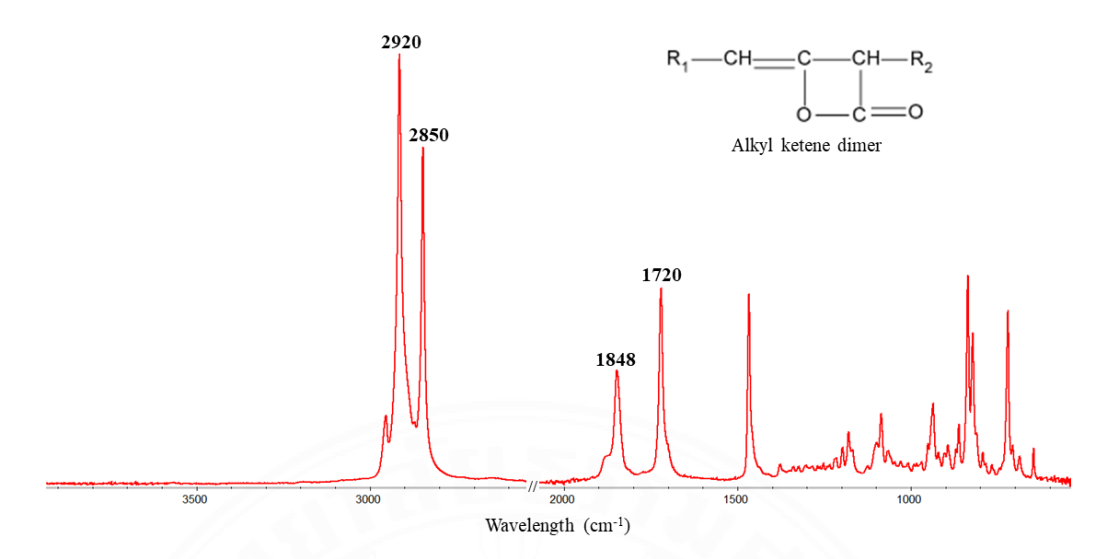


Figure 4.5 FTIR spectrum of neat AKD.

There are 2 steps in the cellulose surface modification process. The MCC was treated with AKD in a ball-milling machine and then heated in an oven at 110 °C for 15 h. The first step allowed for the good mixing of AKD with cellulose without using a solvent. The two opponents were mixed in a dry state. The ball-milling was used to homogenize the mixture by various mechanical stresses such as impact, compression, friction, and shear to cause the well-mixing between AKD and cellulose fiber (Sitotaw et al., 2021).

The second step is for the generated reaction between AKD and cellulose fiber by heating at 110 °C for 15 h. Yuan and Wen (2018) suggested that the temperature for increasing the reaction between the AKD and cellulose fiber is around 70 - 110 °C.



**Figure 4.6** The chemical reaction of AKD-treated cellulose surface.

The chemical reaction among AKD and hydroxyl groups (-OH) of RSC was confirmed by ATR-FTIR spectroscopy. The spectra of AKD-treated cellulose from different reaction times are compared in Figure 4.7. The spectrum of the rice straw cellulose with AKD (RSCD) showed a band at 3335 cm<sup>-1</sup>, corresponding to the -OH groups of cellulose. The two strong bands at 2920 and 2850 cm<sup>-1</sup> in neat AKD, corresponding to the stretching vibrations of C-H in methylene and methyl groups of AKD tails, are present in all spectra. The two bands at 1848 and 1720 cm<sup>-1</sup> correspond to C=O in the lactone ring, and C=C is connected to the lactone ring of AKD. The peak at 1848 cm<sup>-1</sup> is observed from the products treated at the first 5 h reaction time. However, this band completely disappeared after 15 h treatment time, simultaneously forming a new band at 1735 cm<sup>-1</sup> of C=O of linear ester, confirming the successful grafting of AKD, generating a β-ketoester bond on the cellulose surface.

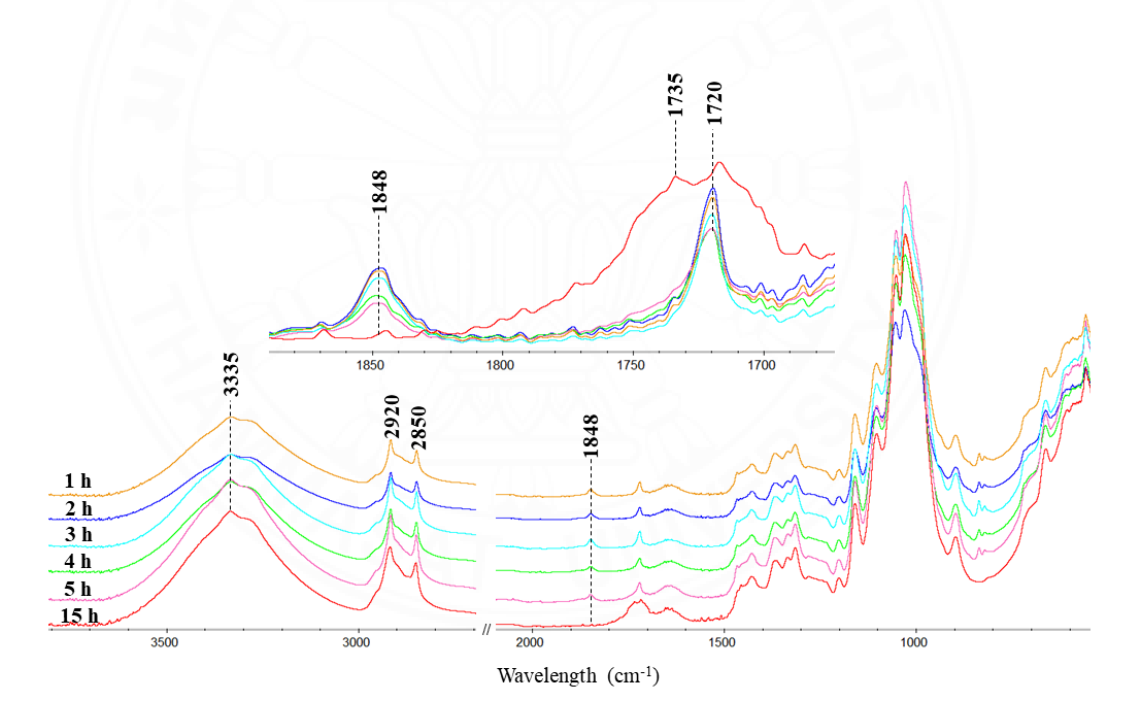


**Figure 4.7** ATR-FTIR spectra of MCCD various reaction times.

The RSC is then treated with AKD at the optimum conditions from the previous screening experiment. The reaction time for allowing reaction among -OH of cellulose and lactone ring of AKD after the ball-milling process at 15 h and 110 °C was chosen. The spectra of neat AKD, RSC, RSCD after ball milling, and RSCD after heating at 110 °C are compared in Figure 4.8. It is observed that a new forming  $\beta$ -ketoester bond

is detected at 1735 cm<sup>-1</sup>. This may lead to lower hydrogen bonding in the cellulose structures (Ali Varshoei, 2013; Kaewsaneha et al., 2022).

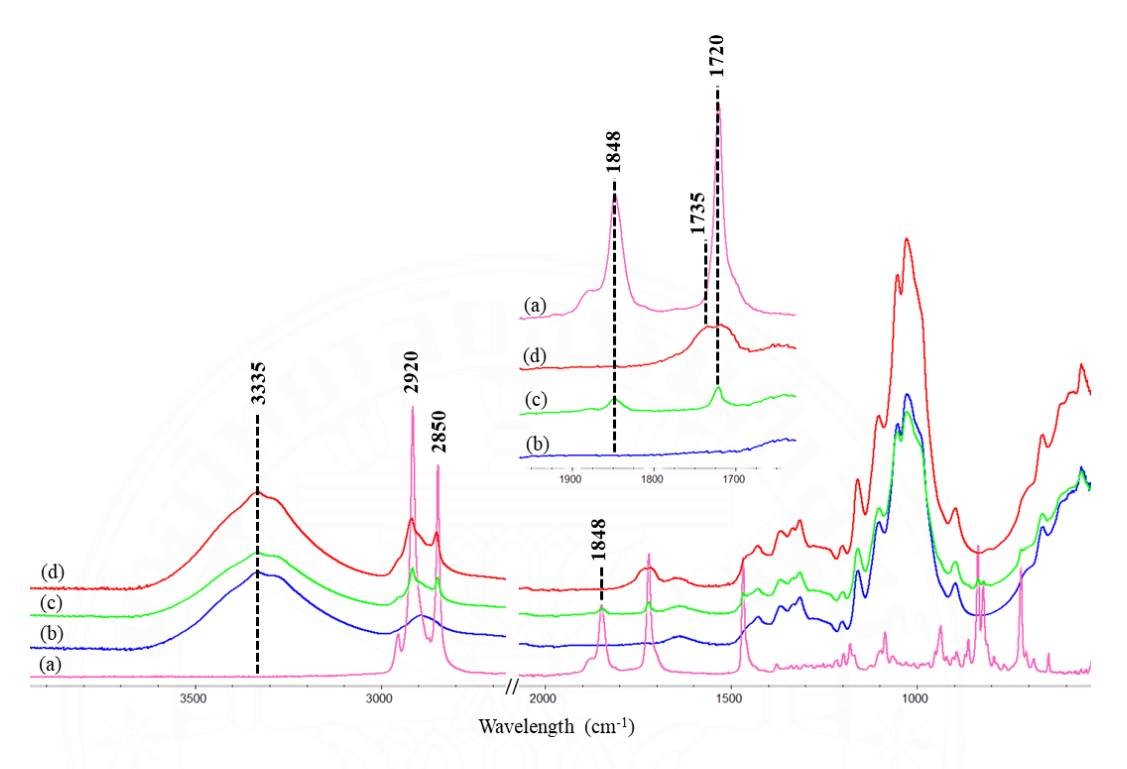


**Figure 4.8** ATR-FTIR spectra of (a) neat AKD, (b) RSC, (c) RSCD after ball milling, and (d) RSCD after heating at 110 °C.

The stability of the grafting AKD is further investigated by dissolving the treated fibers in THF, and the washed sample is coded as RSCT. The FTIR spectra of washed and unwashed samples are recorded and compared in Figure 4.9. It is clearly observed that some hydrophobic tails from an excess AKD are removed, as reflected by a decrease intensity of the 2920 and 2850 cm<sup>-1</sup> bands and the  $\beta$ -ketoester band at 1735 cm<sup>-1</sup>. This confirmed that AKD is strongly bound to a cellulose surface.

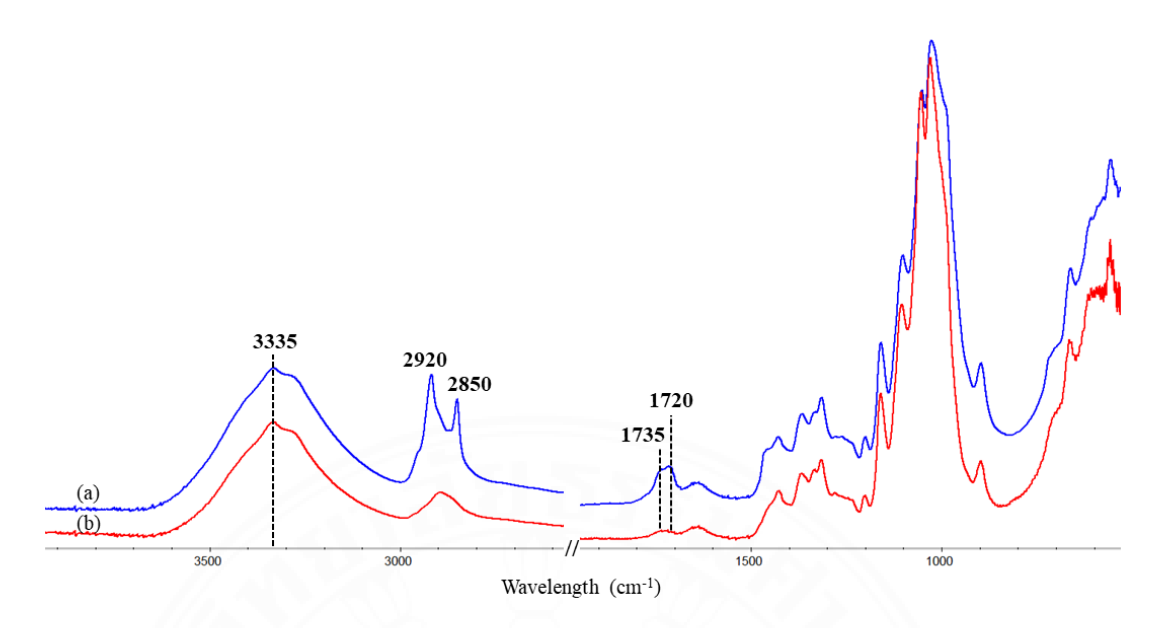
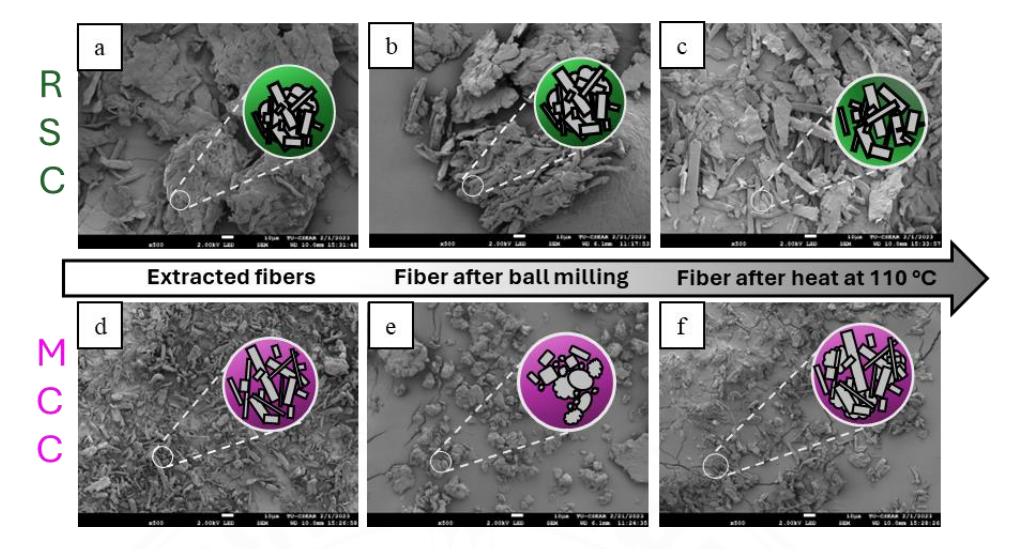


Figure 4.9 ATR-FTIR spectra of (a) RSCD before and (b) after washing with THF.

The surface morphology of the native rice straw, extracted rice straw cellulose, and modified cellulose are studied using SEM. The morphology of the samples before and after AKD treatment are compared in Figure 4.10. The particle size distribution of the modified and unmodified cellulose is determined by the image-J software. The particle size of RSC, RSC after ball milling, RSCD after heating at 110 °C, MCC, MCC after ball milling, and MCCD after heating at 110 °C are 16.1  $\pm$  22.5, 15.9  $\pm$  26.2, 7.4  $\pm$  5.4, 3.3  $\pm$  1.8, 6.5  $\pm$  5.7, and 3.5  $\pm$  2.1  $\mu$ m, respectively. The RSC and RSC after ball milling were largely agglomerated, whereas well-separated particles were observed in RSCD after heating at 110 °C. This suggests that AKD can serve as a surface-modifying agent for cellulose by coating its surface and forming chemical bonds between the lactone ring of AKD and the hydroxyl groups of cellulose. In addition, the MCC and MCC, after ball milling, showed the results of different shapes and separated particles. The MCC were separated better than MCC after ball milling, while small agglomerated and uncertain shapes particles were represented in MCC after ball milling. This corresponds to that without AKD and pressure force from the grinding balls during ball milling, making MCC agglomerate. On the other hand, the MCCD after heating at 110 °C were better separated than the MCC after ball milling, with AKD coating on the surface of the MCCD as though the results of RSCD after heating at 110 °C.



**Figure 4.10** SEM images of (a) RSC, (b) RSC after ball milling, (c) RSCD after heating at 110 °C, (d) MCC, (e) MCC after ball milling, and (f) MCCD after heating at 110 °C.

# Part III Fabrication and characterization of PLA/RSC bio-composite films

The solvent casting method is the most simple method for the fabrication of PLA bio-composite films. The PLA (matrix) and cellulose (reinforcement) are mixed in a solvent by stirring at room temperature, and then the mixed solution is cast on a plate. The uniform film takes shape after the solvent evaporates (Xu et al., 2024). This method significantly influenced the mechanical properties of the composite materials. Bharimalla et al. (2019) reported that composite materials prepared using the solvent casting method exhibited superior results compared to the melt extrusion method, owing to the enhanced dispersion of cellulose and the potential for hydrogen bonding between the reinforcement and the matrix. Moreover, many other factors affect the mechanical properties of composite materials, such as the distribution, shape, size of particles, surface area, orientation, the nature of filler, interfacial interaction, chemical structure, polarity, and concentration of matrix and filler (Basavegowda & Baek, 2021). In the study, the PLA/RSC bio-composite films were prepared using the solvent casting method. The contents of cellulose fiber were varied at 1, 3, 5, and 7 % wt. The mechanical properties, morphology, water vapor permeability (WVP), and hydrophobicity (water contact angle) of the PLA/RSC bio-composite films are investigated. The material is aimed at use in smart packaging films. The films are

expected to be completely compostable, biodegradable, and useful for various applications.

The mechanical properties of neat PLA, PLA/Long RSC, and PLA/Short RSC bio-composite films containing different particle loading are compared in Figures 4.11 - 4.14. All samples show a typical characteristic of brittle material in their stress-strain behavior with high tensile strength and low elongation at break (Figure 4.11). With the addition of Long RSC and Short RSC at 1 %wt. content, the tensile strength presented a high value compared to neat PLA and decreased after adding more content. The Young's modulus of PLA/Long RSC bio- composite films showed a high value when adding content at 1 % wt. and then decreased due to the high stiffness of the Long RSC itself (Lu et al., 2014). Meanwhile, Young's modulus of Short RSC showed no trend. Regarding the elongation at break, the Short RSC slightly increased compared to neat PLA. In contrast, the Long RSC showed elongation at break lower than neat PLA due to the Long RSC having a shape and size similarly long fiber as shown in Figure 4.2 e, the length is 10 times of Short RSC. This is indicated to the agglomeration and poor distribution of Long RSC in PLA matrix (Paul et al., 2021). This is the reason to choose the Short RSC to keep using waste materials to create a good quality product and modify the surface for study in the next part.

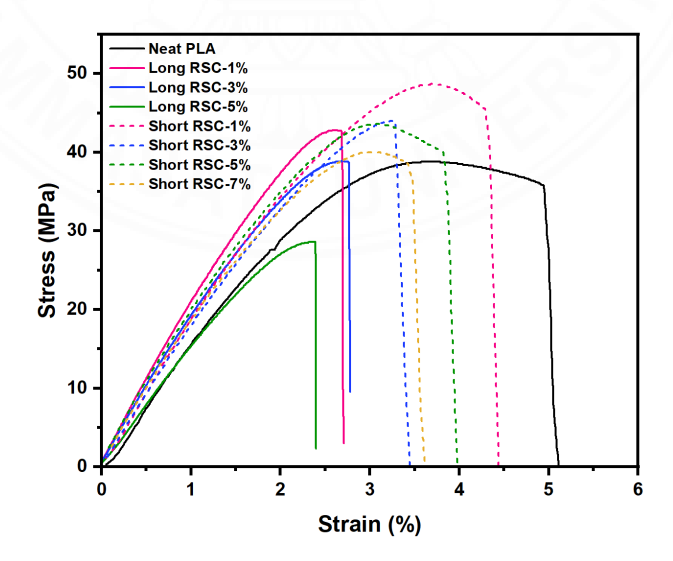


**Figure 4.11** Stress-strain curves of PLA/long and short RSC bio-composite films at various fiber contents.

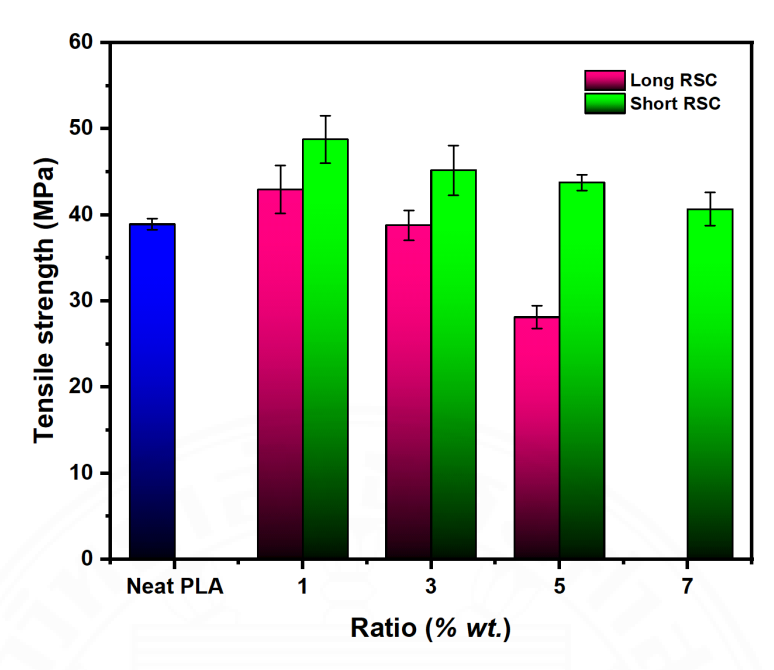


**Figure 4.12** Tensile strength of PLA/long and short RSC bio-composite films at various fiber contents.

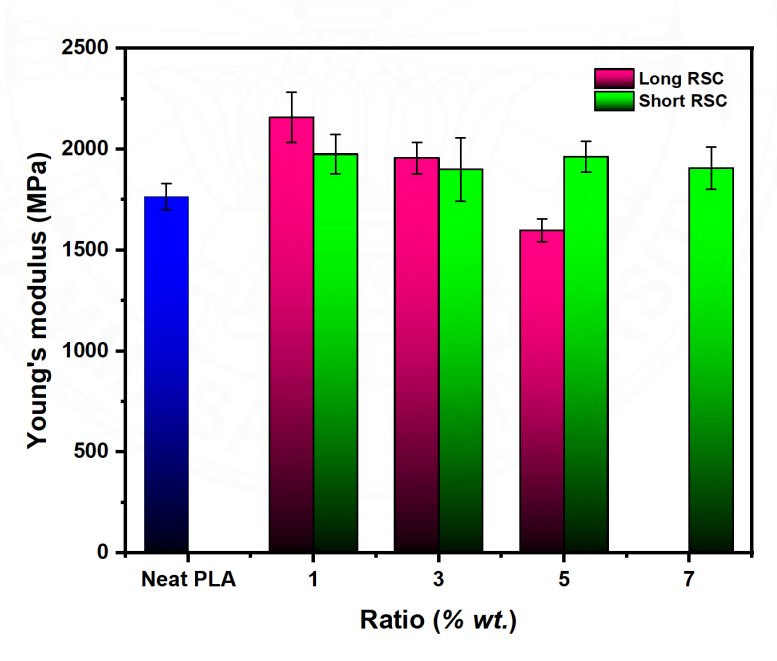


**Figure 4.13** Young's modulus of PLA/long and short RSC bio-composite films at various fiber contents.

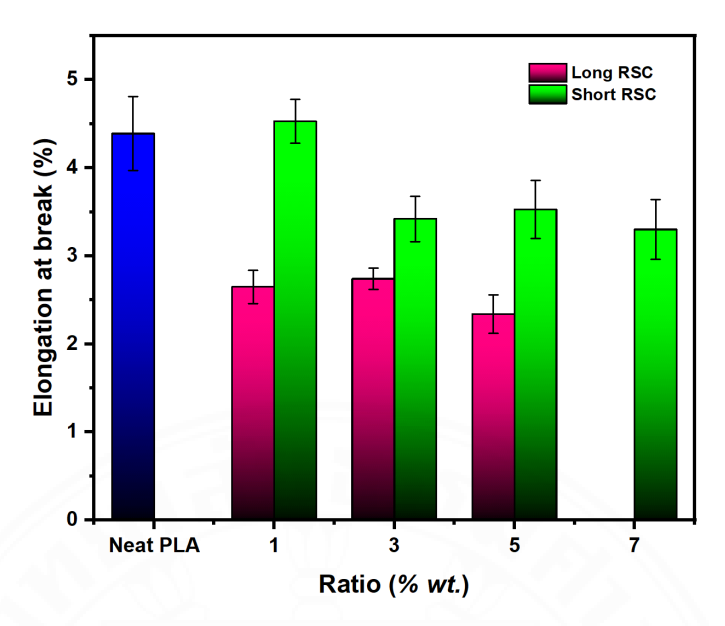


**Figure 4.14** Elongation at break of PLA/long and short RSC bio-composite films at various fiber contents.

The nature of cellulose is hydrophilicity due to the cellulose presenting many -OH groups in the structure. This is an important problem of poor compatibility and interfacial adhesion between cellulose and PLA matrix. The hydroxyl groups of cellulose have a strong attractive force, thereby leading to agglomeration. The agglomeration of cellulose into the polymer matrix directly affects poor mechanical properties. Surface modification of cellulose was a significant method before it was used in composites with a polymer matrix (Mokhena et al., 2018). In this study, modified the RSC surface by employing chemical reactions among -OH groups of cellulose and lactone ring of AKD, improving compatibility between the cellulose fibers and the PLA matrix.

The mechanical properties of neat PLA, PLA/RSC, PLA/RSCD, and AKD biocomposite films containing different particle loading are compared in Figures 4.15 – 4.18. The neat PLA, PLA/RSC, and PLA/RSCD bio-composite films show a typical characteristic of brittle material in their stress-strain behavior with high tensile strength and low elongation at break (Figure 4.15). On the contrary, the PLA/AKD biocomposite films show a typical characteristic of elastic material in their stress-strain behavior with high elongation at break. The bio-composite films show increased tensile strength upon adding 1% of RSC or RSCD. However, the strength linearly decreased

with the increasing fiber content. The maximum strength value of 48.8 and 49.1 MPa was observed for RSC and RSCD composites, respectively, which are 26.8% and 27.6% higher than neat PLA. This is because the cellulose reinforcements are attributed to the hardening of the composite, allowing a transfer of stress to fillers in the domain (Lu et al., 2014). However, no trend is observed in all samples regarding the tensile modulus at all particle loading, but they have slightly better stiffness than neat PLA. In terms of the elongation at break, the samples containing RSCD showed a slight increase at 3 %wt. loading for the AKD-treated fiber, in which the value increased to 7.1 % and then decreased. This is likely because the fibers may be randomly oriented in the PLA matrix. Furthermore, the samples containing AKD show an elongation at break similar to those adding RSCD. The increasing elongation at break of PLA/RSCD biocomposite films is because AKD can improve the RSC distribution and enhance interfacial interaction with the PLA matrix than RSC without AKD, as shown in Figure 4.23. The lower elongation values might be due to fiber agglomeration, particularly with the increased loading content of cellulose fibers (Jonoobi et al., 2010). In contrast, no improvement was observed in PLA/RSC without AKD treatment, even with increased particle loading. This is likely because of the brittle nature of PLA and the agglomerating nature of RSC (Paul et al., 2021).

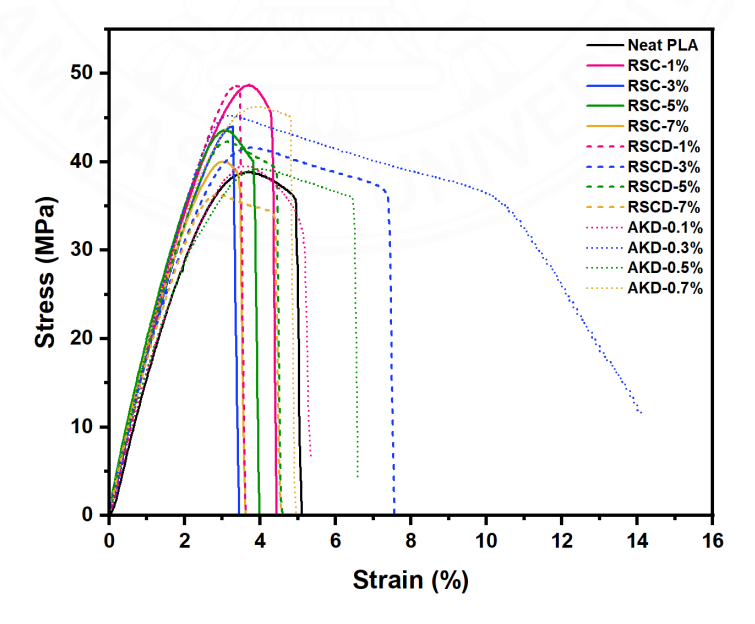


**Figure 4.15** Stress-strain curves of PLA/RSC, RSCD and AKD bio-composite films at various fiber contents.

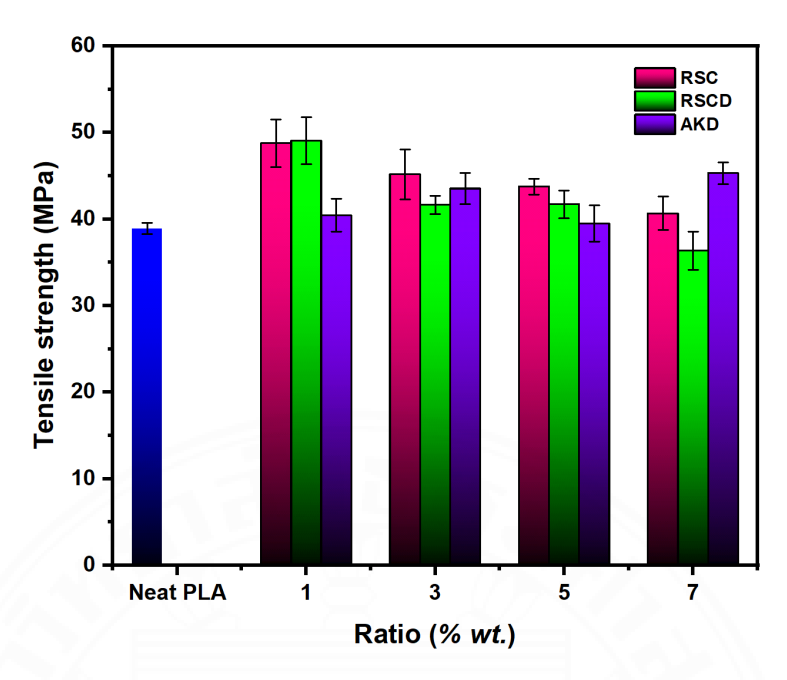


**Figure 4.16** Tensile strength of PLA/RSC, RSCD and AKD bio-composite films at various fiber contents.

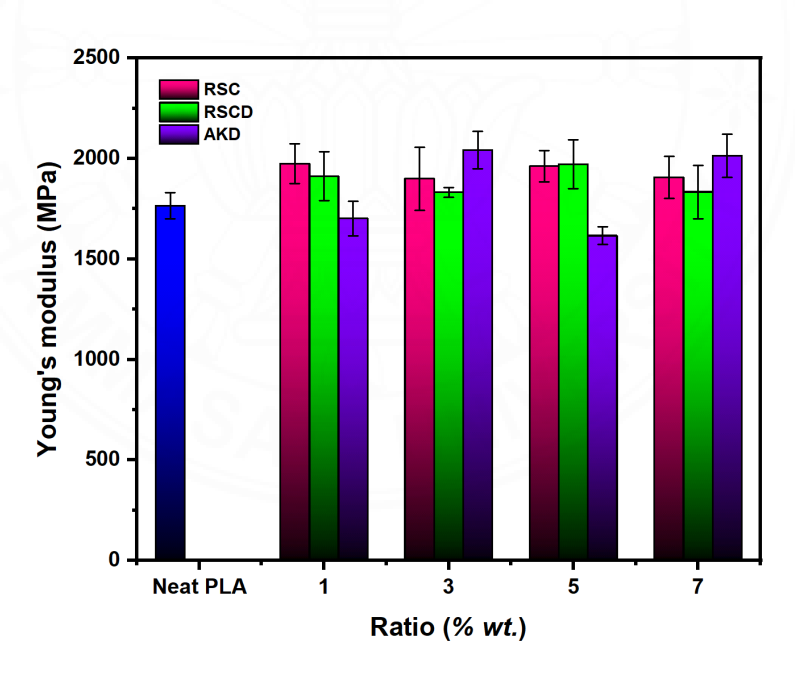


**Figure 4.17** Young's modulus of PLA/RSC, RSCD and AKD bio-composite films at various fiber contents.

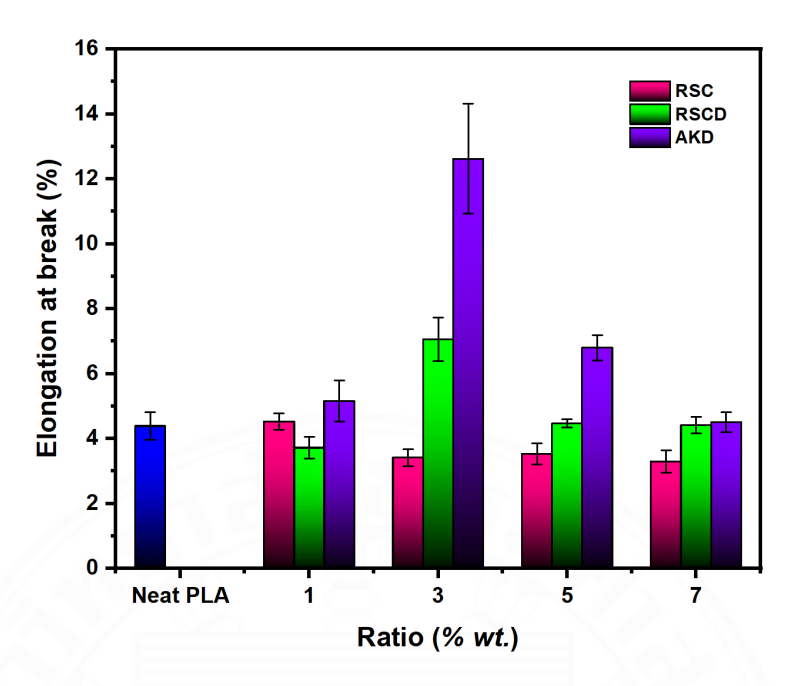


**Figure 4.18** Elongation at break of PLA/RSC, RSCD and AKD bio-composite films at various fiber contents.

Furthermore, the size of particles can also affect the mechanical properties of PLA composites. Abdulkhani et al. (2014) studied PLA nanocomposite films prepared with cellulose nanofiber (CNF) using a solvent-casting method. The surface of CNF was modified to improve the distribution of CNF in the PLA matrix. The materials showed good mechanical properties, especially the elongation at break with the NCF content at 3 and 5 %wt., as the cellulose fiber has nano size, which leads to the good distribution and orientation of nanofiber in the PLA matrix. In this study, the mechanical properties of PLA/RSCD and PLA/MCCD bio-composite films containing different particle loading are compared in Figures 4.19 – 4.22. The PLA/MCCD biocomposite films show a typical characteristic of ductile material in their stress-strain behavior with high elongation at break, especially loading MCCD content at 5 %wt., the highest value is 59.2 MPa. At the same time, PLA/RSCD showed an increase in the elongation at break at 3 %wt. content and then decrease. The particle size of MCCD is smaller than RSCD, as shown in Figure 4.10 c and f, in which the smaller size of cellulose can increase the surface area for more interfacial interaction and distribution in the PLA matrix (Lu et al., 2014). Thus, the good mechanical properties of

PLA/MCCD bio-composite films may indicate the well-interfacial interaction and distribution between MCCD and PLA matrix.

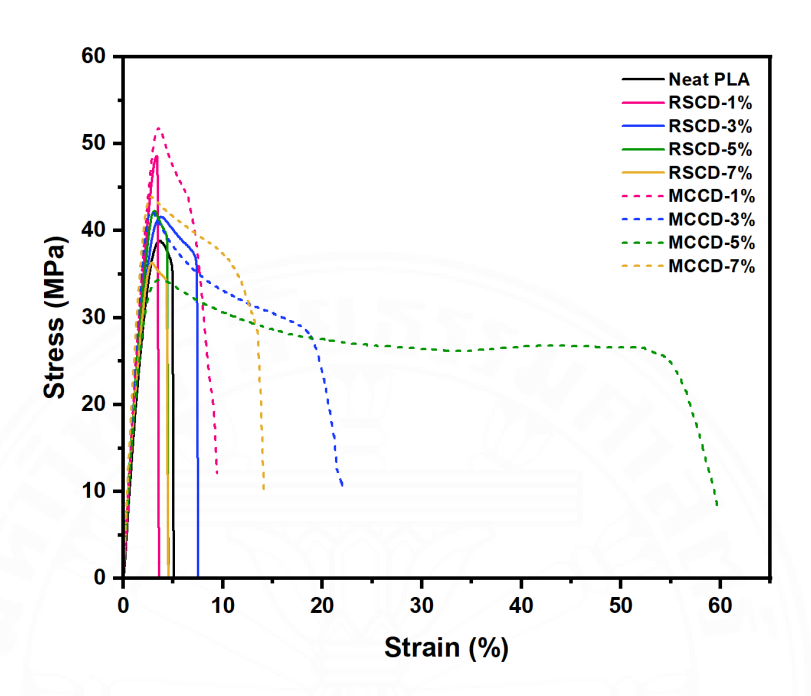


**Figure 4.19** Stress-strain curves of PLA/RSCD and MCCD bio-composite films at various fiber contents.

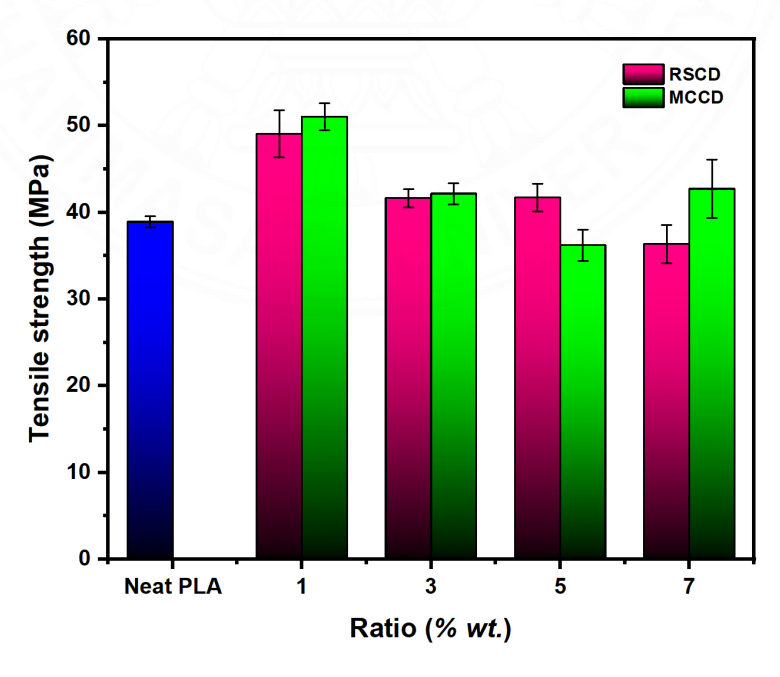


**Figure 4.20** Tensile strength of PLA/RSCD and MCCD bio-composite films at various fiber contents.

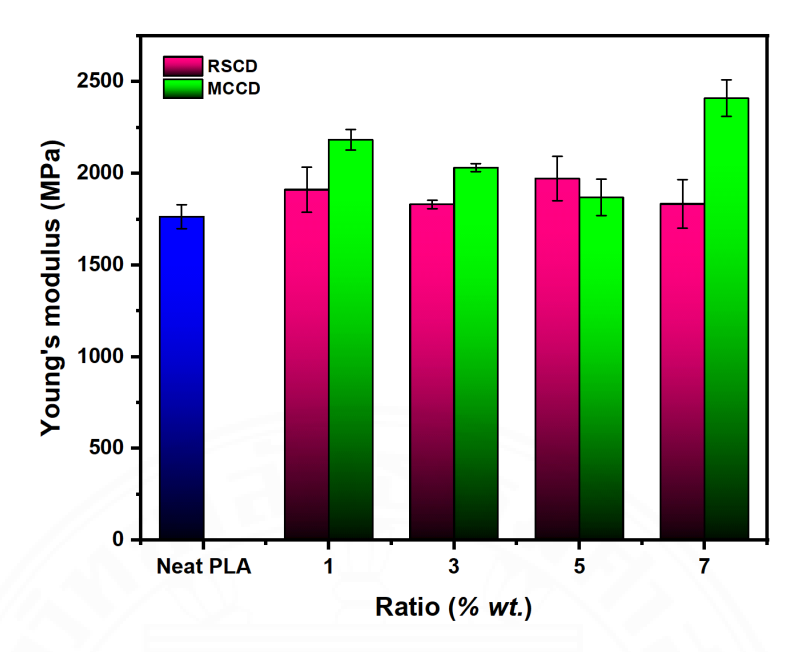


**Figure 4.21** Young's modulus of PLA/RSCD and MCCD bio-composite films at various fiber contents.

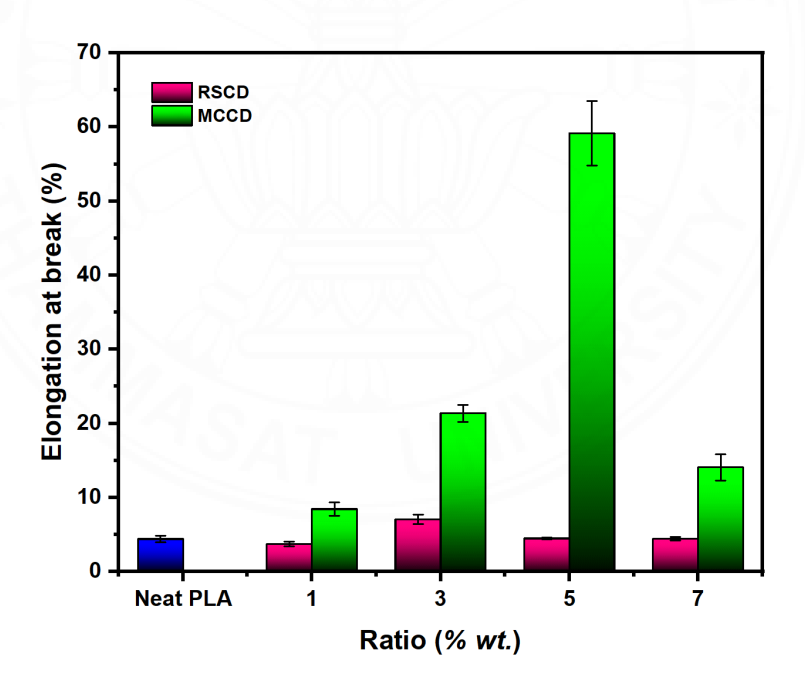


**Figure 4.22** Elongation at break of PLA/RSCD and MCCD bio-composite films at various fiber contents.

The cross-section morphology of PLA/RSC and PLA/RSCD bio-based composite films from the tensile fracture was investigated by SEM, which were PLA/RSC and PLA/RSCD bio-composite at 3 %wt., respectively, as seen in Figure 4.23. The PLA/RSC bio-composite films represent the agglomeration of RSC indicating its poor distribution and interfacial interaction of RSC in the PLA matrix as shown in Figure 4.23 a, b. RSC is hydrophilic and has different polarity to PLA (Lu et al., 2014). In this case, the fracture surface of PLA/RSC bio-composite films shows a large hole of RSC agglomeration after fracture. Moreover, the RSC with AKD can distribute in the PLA matrix more than the RSC without AKD, as shown in Figure 4.23 c, d. The single fiber dispersed in the PLA matrix due to the AKD will serve as both coating agents for cellulose by reaction with the hydroxyl group on the cellulose surface, preventing agglomeration of particles and enhancing the compatibility of PLA/cellulose composite films (Paul et al., 2021).

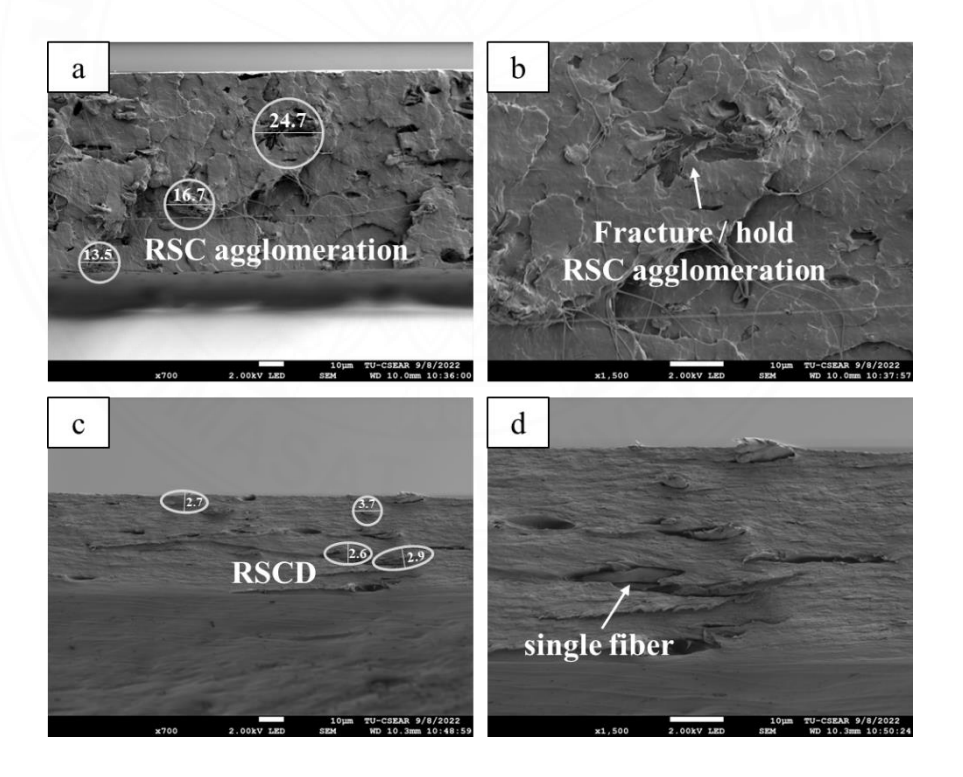


**Figure 4.23** Cross section image of (a, b) PLA/RSC and (c, d) PLA/RSCD bio-based composite films at 3 %wt.

The effect of RSCD on the water barrier and the surface wettability and hydrophobicity of the PLA/RSCD bio-composite films was examined using the water vapor permeability test (WVP) and water contact angle (WCA) measurement. The results are summarized and compared in Figure 4.24 – 4.26, the WVP of neat PLA film is  $7.55 \pm 0.93$  g·mm/m<sup>2</sup>·day. There is no significant change in WVP values at 3 %wt. loading for both RSC and RSCD. The WVP values of PLA/RSC and PLA/RSCD are  $7.65 \pm 1.24$  and  $5.92 \pm 0.89$  g·mm/m<sup>2</sup>·day, respectively. However, upon increasing the particle loading to 7 %wt., the WVP value increased to  $9.83 \pm 1.76 \text{ g} \cdot \text{mm/m}^2 \cdot \text{day}$ . This is likely due to the heterogeneous distributions of RSCD in the PLA matrix, which create more microvoids, leading to a higher permeability. (Paul et al., 2021). The hydrophobicity of PLA/RSCD bio-composite films was examined. The WCA value of the PLA/RSC bio-composite films at all RSC loading is similar to neat PLA, in which the values are in the range of 72.3-74.1°. These results proved that the WCA values remain almost constant regardless of the RSC content. In contrast, the value of films containing RSCD increased to  $91.5 \pm 4.7^{\circ}$  at 7 %wt. This confirms that adding RSCD improves the surface hydrophobicity of PLA as part of AKD, and RSCD may migrate to/and stay at the surface.

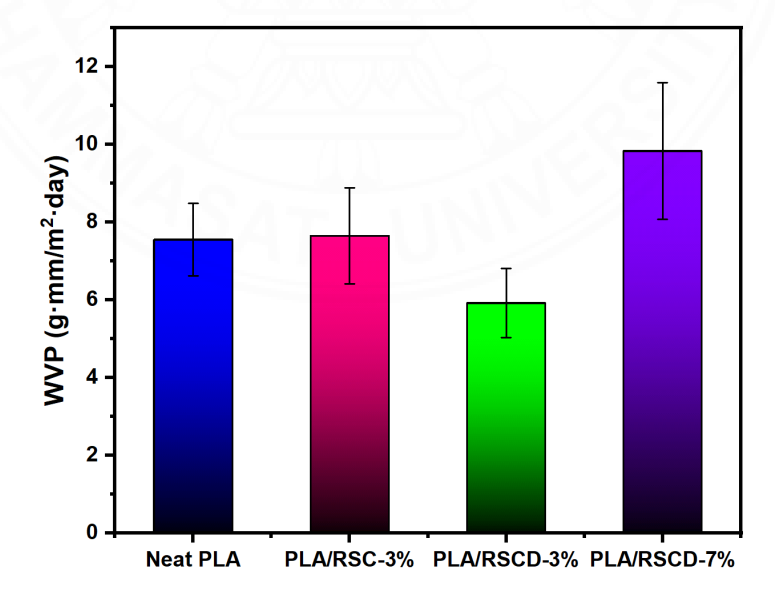


**Figure 4.24** Water vapor permeability of PLA/RSC bio-composite films at various fiber contents.

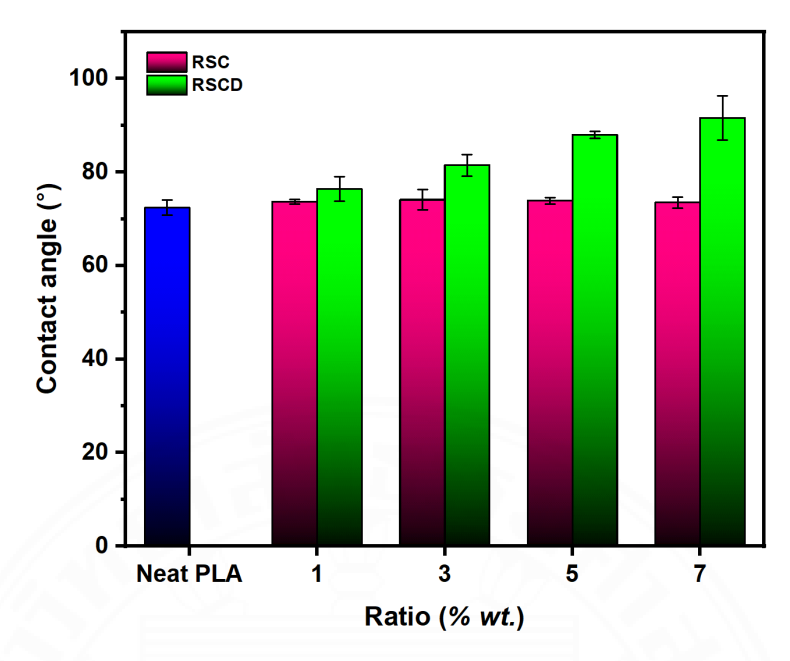


**Figure 4.25** Water contact angle of PLA/RSC and RSCD bio-composite films at various fiber contents.

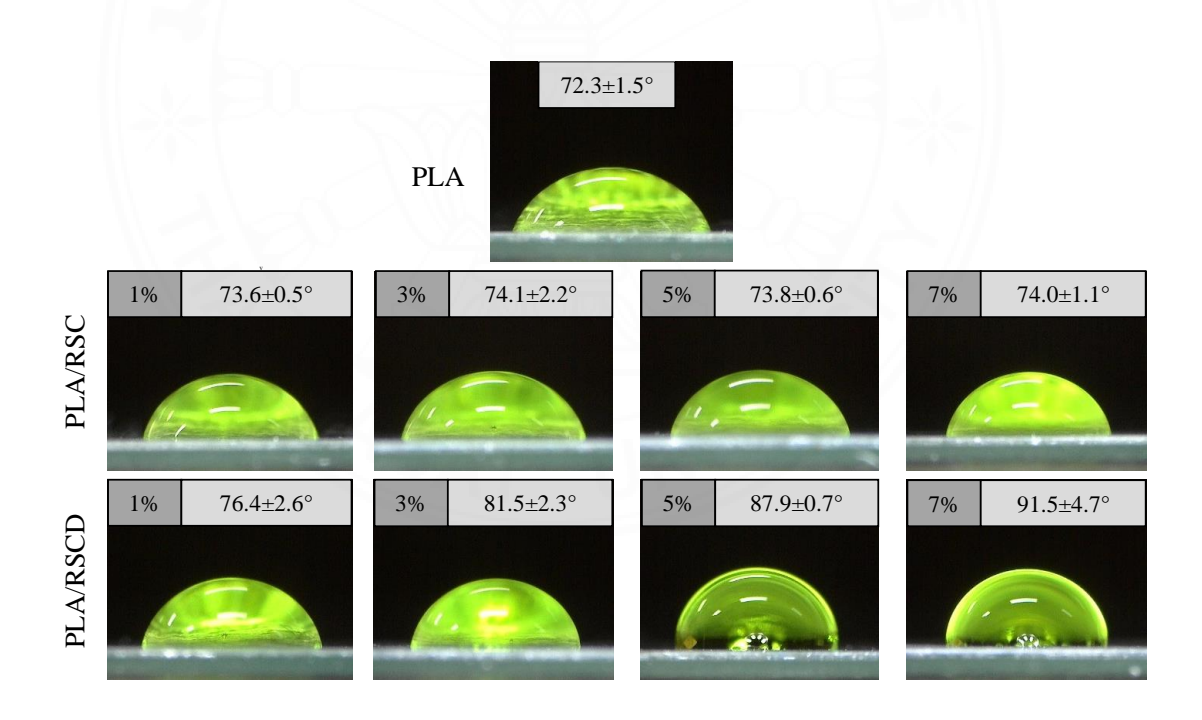


**Figure 4.26** WCA images of PLA/RSC and RSCD bio-composite films at various RSC contents.

#### CHAPTER 5

## CONCLUSIONS AND RECOMMENDATIONS

# **5.1 Conclusions**

Rice straw cellulose (RSC) was successfully extracted by chemical treatment from rice straw (RS). The cellulose fibers obtained from these methods have a diameter of  $7.4 \pm 5.4 \,\mu m$ . RSC was then modified through a solvent-free process ball-milling technique in the presence of AKD to induce the reaction between AKD and RSC. The chemical reaction led to chemical bonding between the lactone ring of AKD and hydroxyl groups of the RSC to form  $\beta$ -ketoester bonds when heated at a temperature of 110 °C for 15 h on the RSCD surface. The morphology studies of RSCD showed relatively good fiber separation with a lower degree of accumulation due to the presence of hydrophobic AKD molecules on the fiber surface. The PLA/RSC bio-composite films with different concentrations from 0-7 wt.% were produced using the solvent casting method. The incorporation of RSCD did not have a significant effect on the permeability of films. Nonetheless, the increase of the RSCD ratio in a polymer composite exhibited the compatibility of the RSCD, leading to significantly improved hydrophobicity on the surface. In addition, the composites containing 3 %wt RSCD showed a slight increase in elongation at break, likely due to a good distribution of the fibers. However, other factors, e.g., the fiber orientation and the L/D ratios, may also play some role. Further study will be conducted to examine the origin of this phenomenon. Nonetheless, the materials have a high potential as smart packaging films.

#### **5.2 Suggestions and Recommendations**

- 1. Reducing the size of RSC to nanoscale through enhanced reaction conditions or elevated chemical concentration.
- 2. Modification of RSCD through various amounts of AKD until the hydroxyl group is reduced or removed to enhance hydrophobicity and compatibility with PLA matrix.

#### REFERENCES

- Abdulkhani, A., Hosseinzadeh, J., Ashori, A., Dadashi, S., & Takzare, Z. (2014). Preparation and characterization of modified cellulose nanofibers reinforced polylactic acid nanocomposite. *Polymer Testing*, 3 5 , 7 3 7 9 . https://doi.org/10.1016/j.polymertesting.2014.03.002
- Ali Varshoei, E. J., Mehdi Rahmaninia and Farhad Rahmany. (2013). The Performance of Alkylketene Dimer (AKD) for the Internal Sizing of Recycled OCC Pulp. *Lignocellulose*, 2(1), 316-326.
- Angin, N., Caylak, S., Ertas, M., & Donmez Cavdar, A. (2022). Effect of alkyl ketene dimer on chemical and thermal properties of polylactic acid (PLA) hybrid composites. *Sustainable Materials and Technologies*, 3 2 . https://doi.org/10.1016/j.susmat.2021.e00386
- Arrieta, M. P., López, J., Rayón, E., & Jiménez, A. (2014). Disintegrability under composting conditions of plasticized PLA–PHB blends. *Polymer Degradation and Stability*, 1 0 8 , 3 0 7 3 1 8 . https://doi.org/10.1016/j.polymdegradstab.2014.01.034
- Basavegowda, N., & Baek, K. H. (2021). Advances in Functional Biopolymer-Based Nanocomposites for Active Food Packaging Applications. *Polymers (Basel)*, 13(23). https://doi.org/10.3390/polym13234198
- Bharimalla, A. K., Patil, P. G., Mukherjee, S., Yadav, V., & Prasad, V. (2019). Nanocellulose-Polymer Composites: Novel Materials for Food Packaging Applications. In *Polymers for Agri-Food Applications* (pp. 553-599). https://doi.org/10.1007/978-3-030-19416-1\_27
- Bordes, P., Pollet, E., & Averous, L. (2009). Nano-biocomposites: Biodegradable polyester/nanoclay systems. *Progress in Polymer Science*, 34(2), 125-155. https://doi.org/10.1016/j.progpolymsci.2008.10.002
- Caylak, S., Ertas, M., Donmez Cavdar, A., & Angin, N. (2021). Mechanical characteristics and hydrophobicity of alkyl ketene dimer compatibilized hybrid biopolymer composites. *Polymer Composites*, 42(5), 2324-2333. https://doi.org/10.1002/pc.25980
- Chen, M., Ma, Y., Xu, Y., Chen, X., Zhang, X., & Lu, C. (2013). Isolation and Characterization of Cellulose Fibers from Rice Straw and its Application in Modified Polypropylene Composites. *Polymer-Plastics Technology and Engineering*, 5 2 ( 1 5 ) , 1 5 6 6 1 5 7 3 . https://doi.org/10.1080/03602559.2013.824465
- Chirayil, C. J., Joy, J., Mathew, L., Mozetic, M., Koetz, J., & Thomas, S. (2014). Isolation and characterization of cellulose nanofibrils from Helicteres isora plant. *Industrial Crops and Products*, 5 9 , 2 7 3 4 . https://doi.org/10.1016/j.indcrop.2014.04.020
- Collard, F.-X., & Blin, J. (2014). A review on pyrolysis of biomass constituents: Mechanisms and composition of the products obtained from the conversion of cellulose, hemicelluloses and lignin. *Renewable and Sustainable Energy Reviews*, 38, 594-608. https://doi.org/10.1016/j.rser.2014.06.013
- Fortunati, E., Peltzer, M., Armentano, I., Torre, L., Jimenez, A., & Kenny, J. M. (2012). Effects of modified cellulose nanocrystals on the barrier and migration

- properties of PLA nano-biocomposites. *Carbohydr Polym*, 90(2), 948-956. https://doi.org/10.1016/j.carbpol.2012.06.025
- He, Y., Ye, H.-C., You, T.-T., & Xu, F. (2023). Sustainable and multifunctional cellulose-lignin films with excellent antibacterial and UV-shielding for active food packaging. *Food Hydrocolloids*, 1 3 7 . https://doi.org/10.1016/j.foodhyd.2022.108355
- Hozman-Manrique, A. S., Garcia-Brand, A. J., Hernandez-Carrion, M., & Porras, A. (2 0 2 3). Isolation and Characterization of Cellulose Microfibers from Colombian Cocoa Pod Husk via Chemical Treatment with Pressure Effects. *Polymers (Basel)*, 15(3). https://doi.org/10.3390/polym15030664
- Huang, P., Wu, M., Kuga, S., Wang, D., Wu, D., & Huang, Y. (2012). One-step dispersion of cellulose nanofibers by mechanochemical esterification in an organic solvent. *ChemSusChem*, 5 (12), 2319-2322. https://doi.org/10.1002/cssc.201200492
- Hundhausen, U., Militz, H., & Mai, C. (2008). Use of alkyl ketene dimer (AKD) for surface modification of particleboard chips. *European Journal of Wood and Wood Products*, 67(1), 37-45. https://doi.org/10.1007/s00107-008-0275-z
- Ilyas, R. A., Sapuan, S. M., Harussani, M. M., Hakimi, M., Haziq, M. Z. M., Atikah, M. S. N., Asyraf, M. R. M., Ishak, M. R., Razman, M. R., Nurazzi, N. M., Norrrahim, M. N. F., Abral, H., & Asrofi, M. (2021). Polylactic Acid (PLA) Biocomposite: Processing, Additive Manufacturing and Advanced Applications. *Polymers (Basel)*, 13(8). https://doi.org/10.3390/polym13081326
- Jaikaew, N., Petchsuk, A., & Opaprakasit, P. (2018). Preparation and Properties of Polylactide Bio-composites with Surface-modified Silica Particles. *Chiang Mai J.* 5, 45.
- Jiang, Z., & Ngai, T. (2022). Recent Advances in Chemically Modified Cellulose and Its Derivatives for Food Packaging Applications: A Review. *Polymers (Basel)*, 14(8). https://doi.org/10.3390/polym14081533
- Johar, N., Ahmad, I., & Dufresne, A. (2 0 1 2). Extraction, preparation and characterization of cellulose fibres and nanocrystals from rice husk. *Industrial Crops and Products*, 3 7 (1), 9 3 9 9. https://doi.org/10.1016/j.indcrop.2011.12.016
- Jonoobi, M., Harun, J., Mathew, A. P., & Oksman, K. (2010). Mechanical properties of cellulose nanofiber (CNF) reinforced polylactic acid (PLA) prepared by twin screw extrusion. *Composites Science and Technology*, 70(12), 1742-1747. https://doi.org/10.1016/j.compscitech.2010.07.005
- Kaewsaneha, C., Roeurn, B., Apiboon, C., Opaprakasit, M., Sreearunothai, P., & Opaprakasit, P. (2022). Preparation of Water-Based Alkyl Ketene Dimer (AKD) Nanoparticles and Their Use in Superhydrophobic Treatments of Value-Added Teakwood Products. *ACS Omega*, 7 (31), 27400-27409. https://doi.org/10.1021/acsomega.2c02420
- Kale, G., Auras, R., & Singh, S. P. (2006). Degradation of Commercial Biodegradable Packages under Real Composting and Ambient Exposure Conditions. *J Polym Environ*, 14, 317-334. https://doi.org/10.1007/s10924-006-0015-6
- Kale, R. D., Gorade, V. G., Madye, N., Chaudhary, B., Bangde, P. S., & Dandekar, P.
   P. (2018). Preparation and characterization of biocomposite packaging film from poly(lactic acid) and acylated microcrystalline cellulose using rice bran

- oil. Int J Biol Macromol, 1 1 8 ( Pt A), 1 0 9 0 1 1 0 2 . https://doi.org/10.1016/j.ijbiomac.2018.06.076
- Kophimai, Y., Cheenacharoen, S., Simister, R., Gomez, L. D., McQueen-Mason, S. J., & Vuttipongchaikij, S. (2020). Straw digestibility of Thai rice accessions. *Agriculture and Natural Resources*, 5 4 , 6 1 7 - 6 2 2 . https://doi.org/10.34044/j.anres.2020.54.6.07
- Kumar, R., Kumari, S., Rai, B., Das, R., & Kumar, G. (2019). Effect of nano-cellulosic fiber on mechanical and barrier properties of polylactic acid (PLA) green nanocomposite film. *Materials Research Express*, 6 ( 1 2 ) . https://doi.org/10.1088/2053-1591/ab5755
- Kumar, S., Chauhan, V. S., & Chakrabarti, S. K. (2016). Separation and analysis techniques for bound and unbound alkyl ketene dimer (AKD) in paper: A review. *Arabian Journal of Chemistry*, 9, S1 6 3 6 S1 6 4 2. https://doi.org/10.1016/j.arabjc.2012.04.019
- Kumari, S. V. G., Pakshirajan, K., & Pugazhenthi, G. (2022). Recent advances and future prospects of cellulose, starch, chitosan, polylactic acid and polyhydroxyalkanoates for sustainable food packaging applications. *Int J Biol Macromol*, 221, 163-182. https://doi.org/10.1016/j.ijbiomac.2022.08.203
- Lai, S.-M., Wu, S.-H., Lin, G.-G., & Don, T.-M. (2014). Unusual mechanical properties of melt-blended poly(lactic acid) (PLA)/clay nanocomposites. *European Polymer Journal*, 5 2 , 1 9 3 2 0 6 . https://doi.org/10.1016/j.eurpolymj.2013.12.012
- Lan, L., Chen, H., Lee, D., Xu, S., Skillen, N., Tedstone, A., Robertson, P., Garforth, A., Daly, H., Hardacre, C., & Fan, X. (2022). Effect of Ball-Milling Pretreatment of Cellulose on Its Photoreforming for H2 Production. *ACS Sustainable Chemistry & Engineering*, 10 (15), 4862-4871. https://doi.org/10.1021/acssuschemeng.1c07301
- Lu, P., & Hsieh, Y. L. (2012). Preparation and characterization of cellulose nanocrystals from rice straw. *Carbohydr Polym*, 8 7 (1), 5 6 4 5 7 3. https://doi.org/10.1016/j.carbpol.2011.08.022
- Lu, T., Liu, S., Jiang, M., Xu, X., Wang, Y., Wang, Z., Gou, J., Hui, D., & Zhou, Z. (2014). Effects of modifications of bamboo cellulose fibers on the improved mechanical properties of cellulose reinforced poly(lactic acid) composites. *Composites Part B: Engineering*, 6 2 , 1 9 1 1 9 7 . https://doi.org/10.1016/j.compositesb.2014.02.030
- Marano, S., Laudadio, E., Minnelli, C., & Stipa, P. (2022). Tailoring the Barrier Properties of PLA: A State-of-the-Art Review for Food Packaging Applications. *Polymers (Basel)*, 14(8). https://doi.org/10.3390/polym14081626
- Mohamad Haafiz, M. K., Eichhorn, S. J., Hassan, A., & Jawaid, M. (2013). Isolation and characterization of microcrystalline cellulose from oil palm biomass residue. *Carbohydr Polym*, 9 3 ( 2 ) , 6 2 8 6 3 4 . https://doi.org/10.1016/j.carbpol.2013.01.035
- Mohamed, M. A., Abd Mutalib, M., Mohd Hir, Z. A., MF, M. Z., Mohamad, A. B., Jeffery Minggu, L., Awang, N. A., & WN, W. S. (2017). An overview on cellulose-based material in tailoring bio-hybrid nanostructured photocatalysts for water treatment and renewable energy applications. *Int J Biol Macromol*, 103, 1232-1256. https://doi.org/10.1016/j.ijbiomac.2017.05.181

- Mohanty, A. K., Misra, M., & Hinrichsen, G. (2000). Biofibres, biodegradable polymers and biocomposites: An overview. *Macromol. Mater. Eng.*, 276/277, 1–24.
- Mokhena, T. C., Sefadi, J. S., Sadiku, E. R., John, M. J., Mochane, M. J., & Mtibe, A. (2 0 1 8). Thermoplastic Processing of PLA/Cellulose Nanomaterials Composites. *Polymers (Basel)*, 10(12). https://doi.org/10.3390/polym10121363
- Mondragon, G., Fernandes, S., Retegi, A., Peña, C., Algar, I., Eceiza, A., & Arbelaiz, A. (2014). A common strategy to extracting cellulose nanoentities from different plants. *Industrial Crops and Products*, 5 5 , 1 4 0 1 4 8 . https://doi.org/10.1016/j.indcrop.2014.02.014
- Morán, J. I., Alvarez, V. A., Cyras, V. P., & Vázquez, A. (2007). Extraction of cellulose and preparation of nanocellulose from sisal fibers. *Cellulose*, 15(1), 149-159. https://doi.org/10.1007/s10570-007-9145-9
- Mudgil, D., & Barak, S. (2013). Composition, properties and health benefits of indigestible carbohydrate polymers as dietary fiber: a review. *Int J Biol Macromol*, 61, 1-6. https://doi.org/10.1016/j.ijbiomac.2013.06.044
- Nasri-Nasrabadi, B., Behzad, T., & Bagheri, R. (2014). Extraction and characterization of rice straw cellulose nanofibers by an optimized chemomechanical method. *Journal of Applied Polymer Science*, 1 3 1 ( 7 ) , n/a-n/a. https://doi.org/10.1002/app.40063
- Ncube, L. K., Ude, A. U., Ogunmuyiwa, E. N., Zulkifli, R., & Beas, I. N. (2020). Environmental Impact of Food Packaging Materials: A Review of Contemporary Development from Conventional Plastics to Polylactic Acid Based Materials. *Materials* (*Basel*), 1 3 ( 2 1 ) . https://doi.org/10.3390/ma13214994
- Ng, H.-M., Sin, L. T., Tee, T.-T., Bee, S.-T., Hui, D., Low, C.-Y., & Rahmat, A. R. (2015). Extraction of cellulose nanocrystals from plant sources for application as reinforcing agent in polymers. *Composites Part B: Engineering*, 75, 176-200. https://doi.org/10.1016/j.compositesb.2015.01.008
- Nuruddin, M., Hosur, M., Uddin, M. J., Baah, D., & Jeelani, S. (2015). A novel approach for extracting cellulose nanofibers from lignocellulosic biomass by ball milling combined with chemical treatment. *Journal of Applied Polymer Science*, 133(9). https://doi.org/10.1002/app.42990
- Nuruddin, M., Hosur, M., Uddin, M. J., Baah, D., & Jeelani, s. (2016). A novel approach for extracting cellulose nanofibers from lignocellulosic biomass by ball milling combined with chemical treatment. *Journal of Applied Polymer Science*, 133, 42990. https://doi.org/10.1002/app.42990
- Osman, M. A., & Atia, M. R. A. (2018). Investigation of ABS-rice straw composite feedstock filament for FDM. *Rapid Prototyping Journal*, 24(6), 1067-1075. https://doi.org/10.1108/rpj-11-2017-0242
- Paul, U. C., Fragouli, D., Bayer, I. S., Zych, A., & Athanassiou, A. (2021). Effect of Green Plasticizer on the Performance of Microcrystalline Cellulose/Polylactic Acid Biocomposites. *ACS Applied Polymer Materials*, 3(6), 3071-3081. https://doi.org/10.1021/acsapm.1c00281
- Peelman, N., Ragaert, P., De Meulenaer, B., Adons, D., Peeters, R., Cardon, L., Van Impe, F., & Devlieghere, F. (2013). Application of bioplastics for food

- packaging. *Trends in Food Science & Technology*, 32(2), 128-141. https://doi.org/10.1016/j.tifs.2013.06.003
- Perera, K. Y., Jaiswal, A. K., & Jaiswal, S. (2023). Biopolymer-Based Sustainable Food Packaging Materials: Challenges, Solutions, and Applications. *Foods*, 12(12). https://doi.org/10.3390/foods12122422
- Piras, C. C., Fernández-Prieto, S., & De Borggraeve, W. M. (2019). Ball milling: a green technology for the preparation and functionalisation of nanocellulose derivatives. *Nanoscale Advances*, 1(3), 937-947.
- Popa, E. E., Rapa, M., Popa, O., Mustatea, G., Popa, V. I., Mitelut, A. C., & Popa, M. E. (2017). Polylactic Acid/Cellulose Fibres Based Composites for Food Packaging Applications. *Materiale Plastice*, 54 (4), 673-677. https://doi.org/10.37358/mp.17.4.4923
- Quan, C., Werner, O., Wågberg, L., & Turner, C. (2 0 0 9). Generation of superhydrophobic paper surfaces by a rapidly expanding supercritical carbon dioxide—alkyl ketene dimer solution. *The Journal of Supercritical Fluids*, 49(1), 117-124. https://doi.org/10.1016/j.supflu.2008.11.015
- Ramos, M., Laveriano, E., San Sebastián, L., Perez, M., Jiménez, A., Lamuela-Raventos, R. M., Garrigós, M. C., & Vallverdú-Queralt, A. (2023). Rice straw as a valuable source of cellulose and polyphenols: Applications in the food industry. *Trends in Food Science & Technology*, 1 3 1 , 1 4 2 7 . https://doi.org/10.1016/j.tifs.2022.11.020
- Rathna Priya, T. S., Eliazer Nelson, A. R. L., Ravichandran, K., & Antony, U. (2019). Nutritional and functional properties of coloured rice varieties of South India: a review. *Journal of Ethnic Foods*, 6(1). https://doi.org/10.1186/s42779-019-0017-3
- Reddy, K. O., Uma Maheswari, C., Muzenda, E., Shukla, M., & Rajulu, A. V. (2015). Extraction and Characterization of Cellulose from Pretreated Ficus (Peepal Tree) Leaf Fibers. *Journal of Natural Fibers*, 1 3 (1), 5 4 6 4. https://doi.org/10.1080/15440478.2014.984055
- Rhim, J.-W., Park, H.-M., & Ha, C.-S. (2013). Bio-nanocomposites for food packaging applications. *Progress in Polymer Science*, 38 (10-11), 1629-1652. https://doi.org/10.1016/j.progpolymsci.2013.05.008
- Sheltami, R. M., Abdullah, I., Ahmad, I., Dufresne, A., & Kargarzadeh, H. (2012). Extraction of cellulose nanocrystals from mengkuang leaves (Pandanus tectorius). *Carbohydrate Polymers*, 8 8 (2), 7 7 2 7 7 9. https://doi.org/10.1016/j.carbpol.2012.01.062
- Singh, G., Gupta, M. K., Chaurasiya, S., Sharma, V. S., & Pimenov, D. Y. (2021). Rice straw burning: a review on its global prevalence and the sustainable alternatives for its effective mitigation. *Environ Sci Pollut Res Int*. https://doi.org/10.1007/s11356-021-14163-3
- Sitotaw, Y. W., Habtu, N. G., Gebreyohannes, A. Y., Nunes, S. P., & Van Gerven, T. (2021). Ball milling as an important pretreatment technique in lignocellulose biorefineries: a review. *Biomass Conversion and Biorefinery*. https://doi.org/10.1007/s13399-021-01800-7
- Spiridon, I., Darie, R. N., & Kangas, H. (2016). Influence of fiber modifications on PLA/fiber composites. Behavior to accelerated weathering. *Composites Part B: Engineering*, 92, 19-27. https://doi.org/10.1016/j.compositesb.2016.02.032

- Sudamrao Getme, A., & Patel, B. (2020). A Review: Bio-fiber's as reinforcement in composites of polylactic acid (PLA). *Materials Today: Proceedings*, 26, 2116-2122. https://doi.org/10.1016/j.matpr.2020.02.457
- Talegaonkar, S., Sharma, H., Pandey, S., Mishra, P. K., & Wimmer, R. (2017). Bionanocomposites: smart biodegradable packaging material for food preservation. In *Food Packaging* (pp. 79-110). https://doi.org/10.1016/b978-0-12-804302-8.00003-0
- Wang, H., Sun, X., & Seib, P. (2002). Mechanical properties of poly(lactic acid) and wheat starch blends with methylenediphenyl diisocyanate. *Journal of Applied Polymer Science*, 84(6), 1257-1262. https://doi.org/10.1002/app.10457
- Wen, Y. H., Tsou, C. H., Guzman, M. R. d., Huang, D., Yu, Y. Q., Gao, C., Zhang, X. M., Du, J., Zheng, Y. T., Zhu, H., & Wang, Z. H. (2022). Antibacterial nanocomposite films of poly(vinyl alcohol) modified with zinc oxide-doped multiwalled carbon nanotubes as food packaging. *Polymer Bulletin*, 79, 3847-3866. https://doi.org/10.1007/s00289-021-03666-1
- Xiao, L., Wang, B., Yang, G., & Gauthier, M. (2012). Poly(Lactic Acid)-Based Biomaterials: Synthesis, Modification and Applications. In *Biomedical Science*, *Engineering and Technology*. https://doi.org/10.5772/23927
- Xu, Y., Wu, Z., Li, A., Chen, N., Rao, J., & Zeng, Q. (2024). Nanocellulose Composite Films in Food Packaging Materials: A Review. *Polymers (Basel)*, 16(3). https://doi.org/10.3390/polym16030423
- Yan, J., Liu, J., Sun, Y., Song, G., Ding, D., Fan, G., Chai, B., Wang, C., & Sun, L. (2021). Investigation on the Preparation of Rice Straw-Derived Cellulose Acetate and Its Spinnability for Electrospinning. *Polymers (Basel)*, 13(20). https://doi.org/10.3390/polym13203463
- Yang, Q., Saito, T., & Isogai, A. (2012). Facile fabrication of transparent cellulose films with high water repellency and gas barrier properties. *Cellulose*, 19(6), 1913-1921. https://doi.org/10.1007/s10570-012-9790-5
- Yu, W., Dong, L., Lei, W., Zhou, Y., Pu, Y., & Zhang, X. (2021). Effects of Rice Straw Powder (RSP) Size and Pretreatment on Properties of FDM 3 D-Printed RSP/Poly(Lactic Acid) Biocomposites. *Molecules*, 2 6 ( 1 1 ) . https://doi.org/10.3390/molecules26113234
- Yuan, Z., & Wen, Y. (2018). Enhancement of hydrophobicity of nanofibrillated cellulose through grafting of alkyl ketene dimer. *Cellulose*, 25(12), 6863-6871. https://doi.org/10.1007/s10570-018-2048-0
- Zhang, X., Yang, W., & Blasiak, W. (2011). Modeling Study of Woody Biomass: Interactions of Cellulose, Hemicellulose, and Lignin. *Energy & Fuels*, 25(10), 4786-4795. https://doi.org/10.1021/ef201097d
- Zhou, Y., Hu, Y., Tan, Z., & Zhou, T. (2024). Cellulose extraction from rice straw waste for biodegradable ethyl cellulose films preparation using green chemical technology. *Journal of Cleaner Production*, 4 3 9 . https://doi.org/10.1016/j.jclepro.2024.140839

# **BIOGRAPHY**

Name Supattra Piewkliang

Education 2020: Bachelor of Engineering (Materials Engineering)

Faculty of Engineering

Rajamangala University of Thanyaburi

